



Aalto University
School of Chemical
Technology

CHEM E5125 Thin Film Technology

Lecture 3 PVD 1

Plasma and ion bombardment

Jari Koskinen

jari.koskinen@aalto.fi

17.1.2023

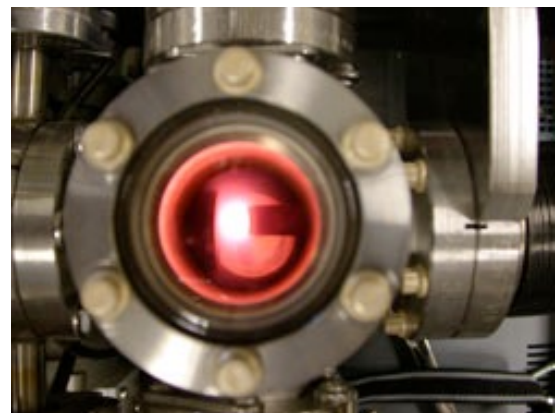
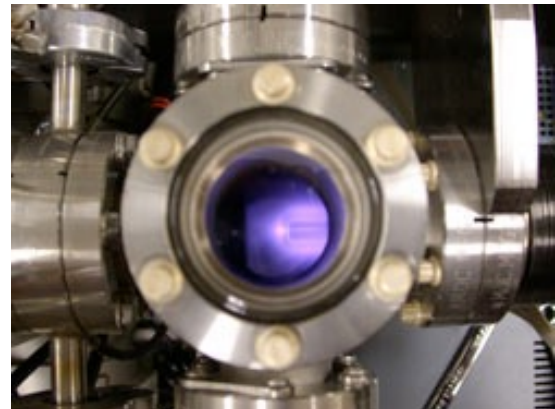
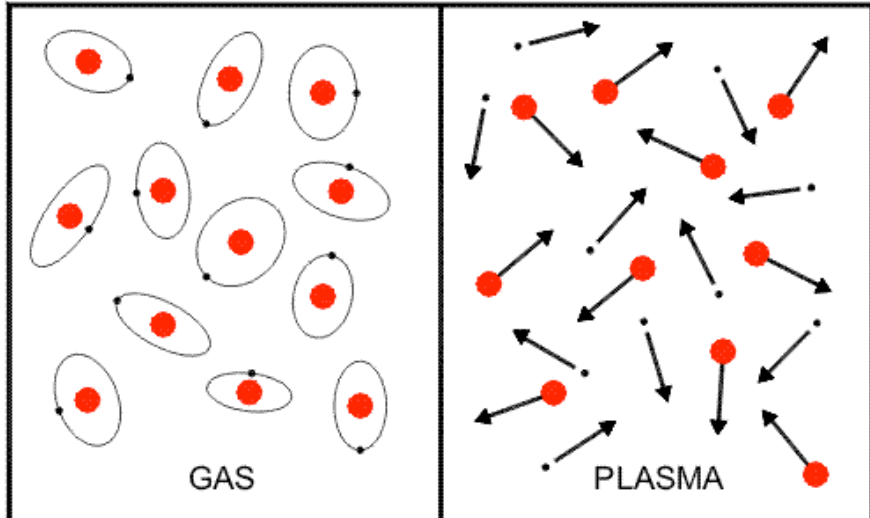
Contents

- Plasma types
- Generation of plasma
- Ion solid interaction
- Thin film microstructure in PVD

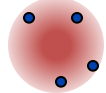
Plasma

- Plasma

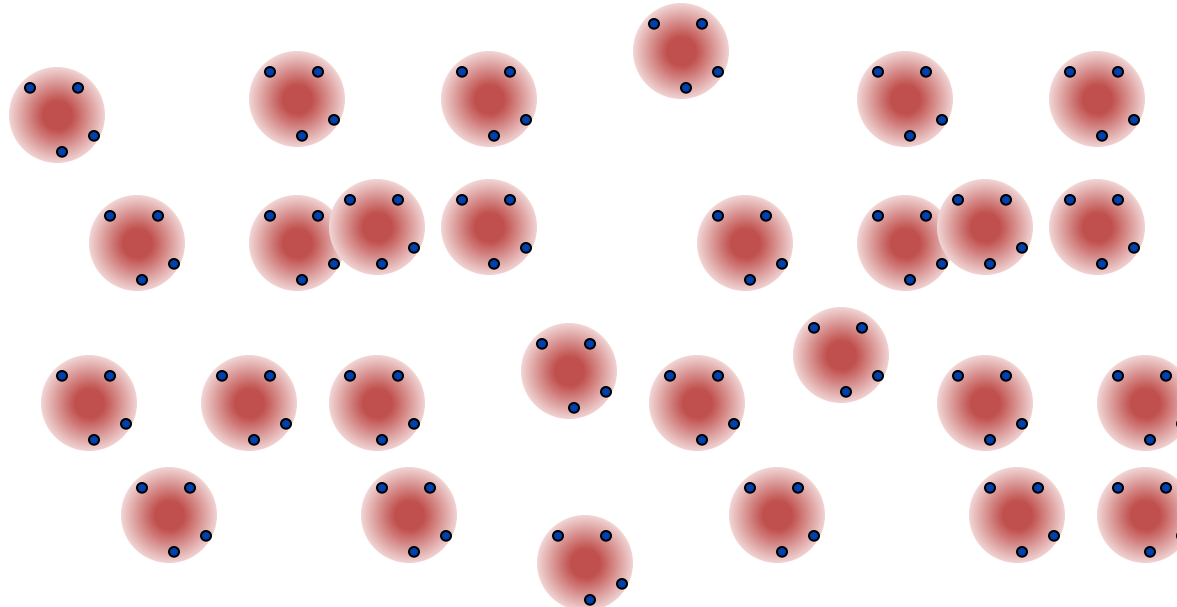
- Gas of positive ions, electrons and (mostly) neutral atoms
- Etymology: Greek: “moulded” - plasma fills the chamber
- Charge neutrality $n_e = n_i$
- Colliding electrons ionise atoms
- Ions and electrons accelerate in electric field
- Collisions excite atoms
-



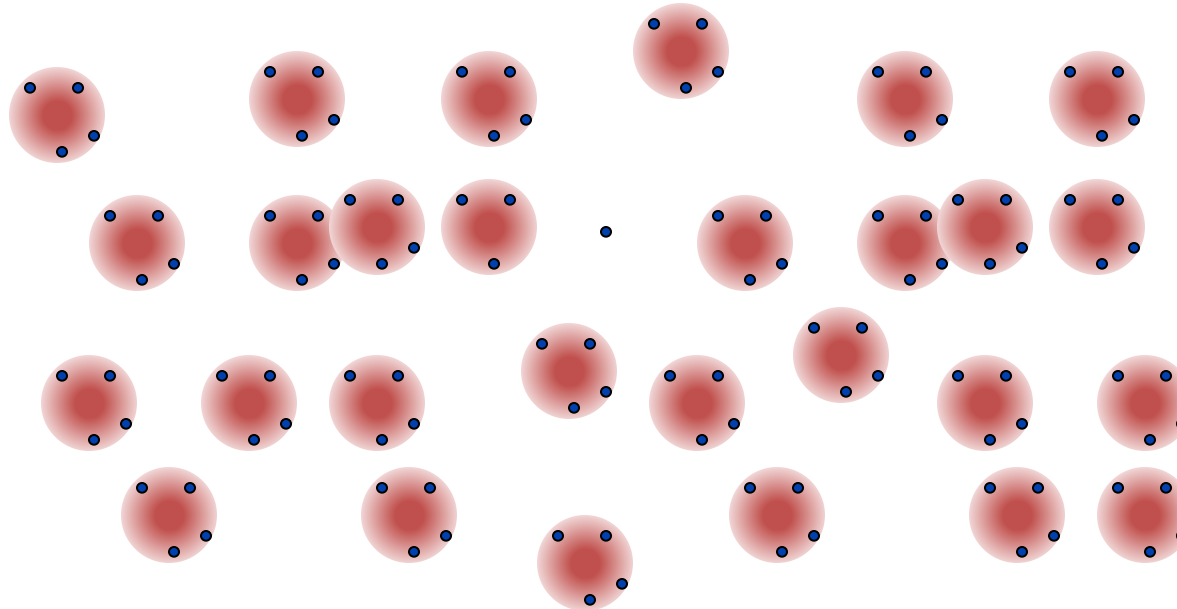
Glow discharge



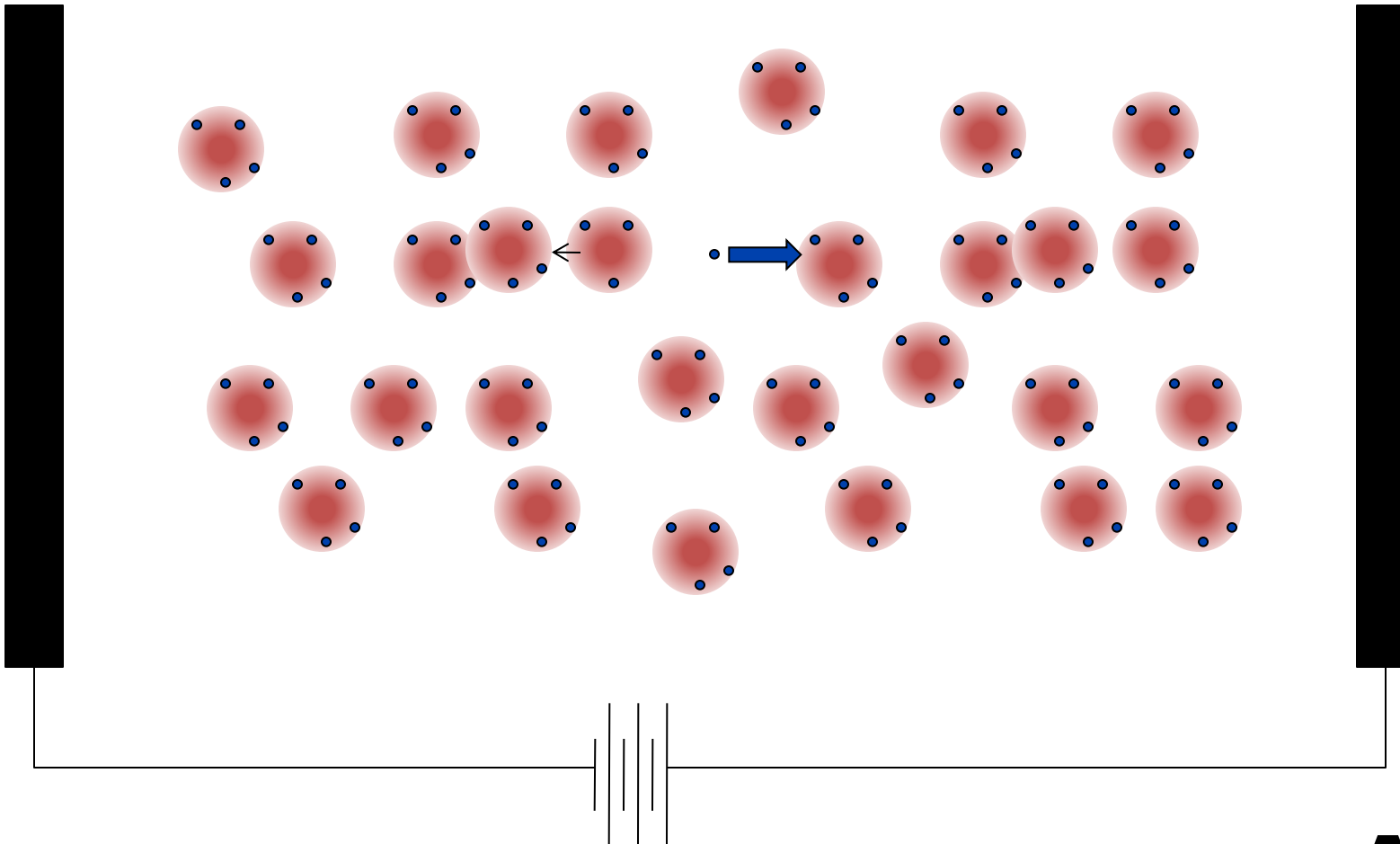
Glow discharge



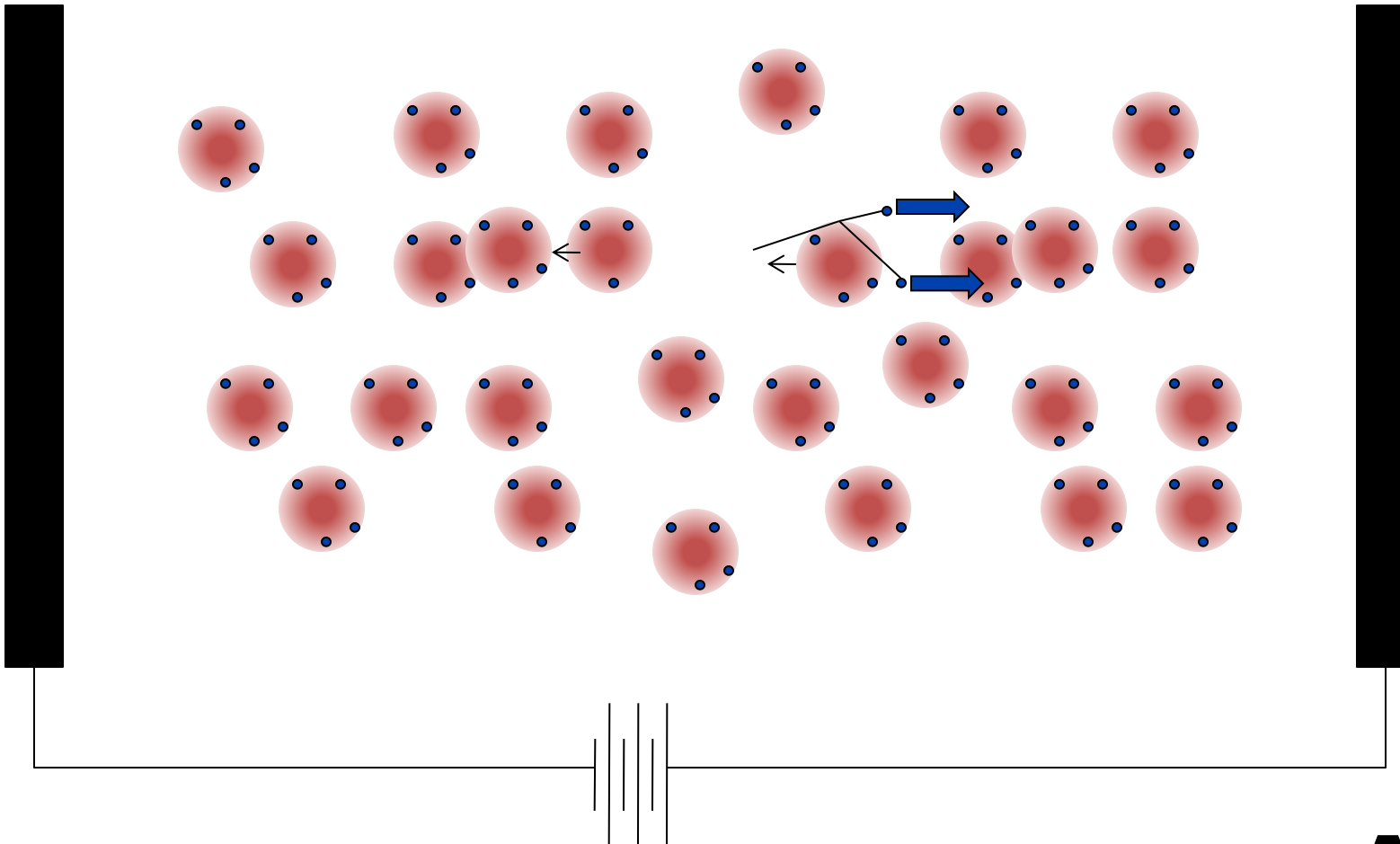
Glow discharge



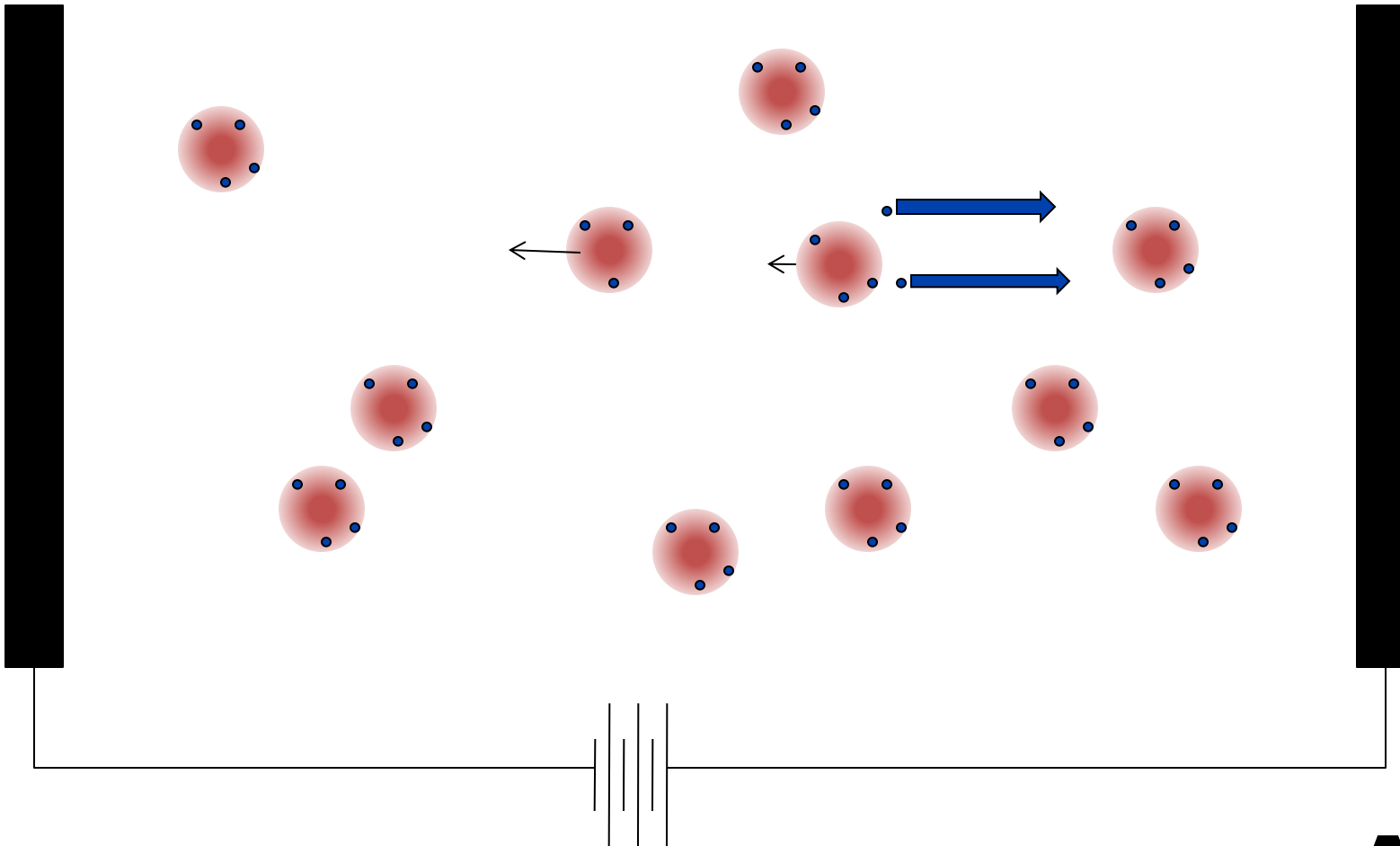
Glow discharge



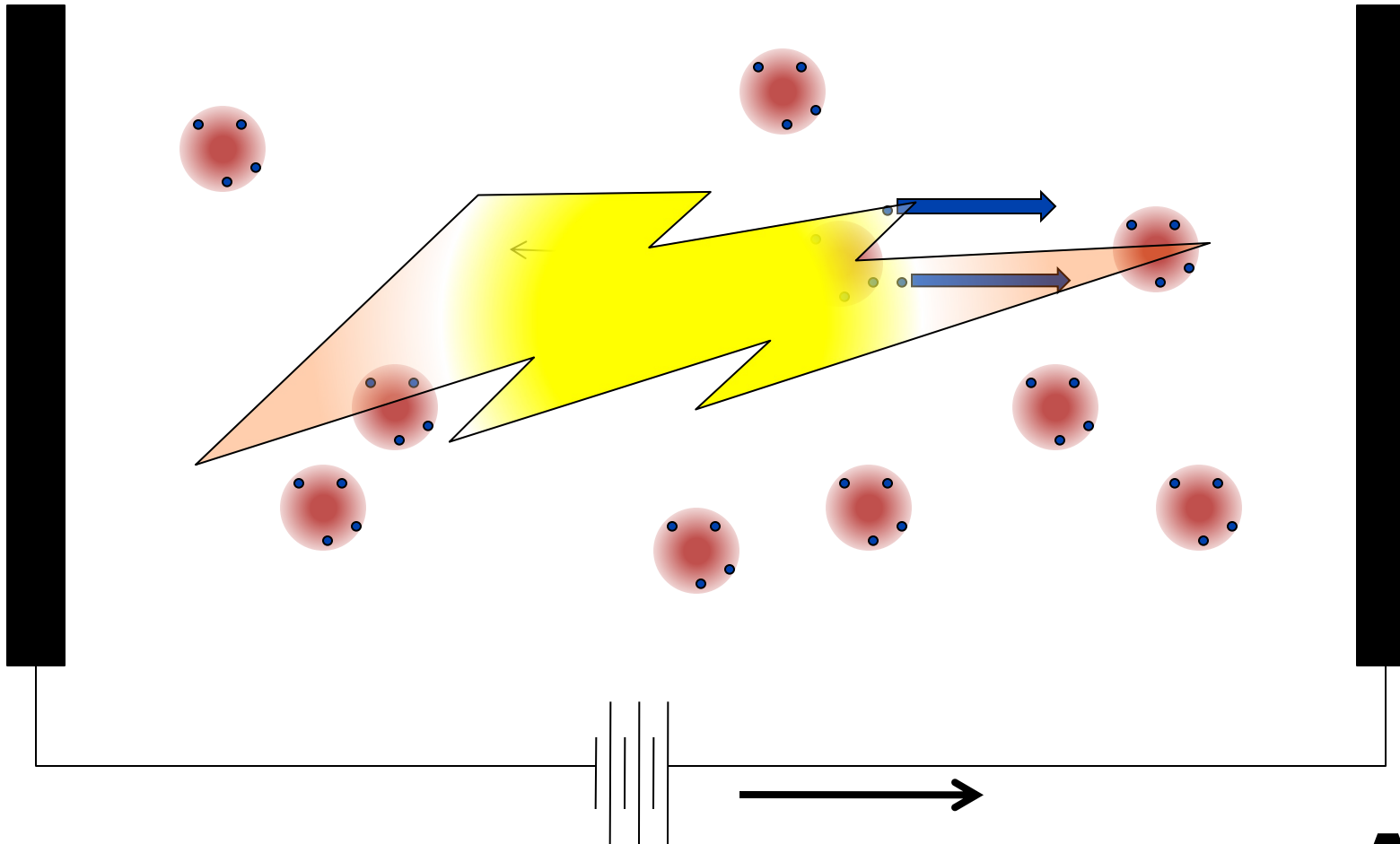
Glow discharge



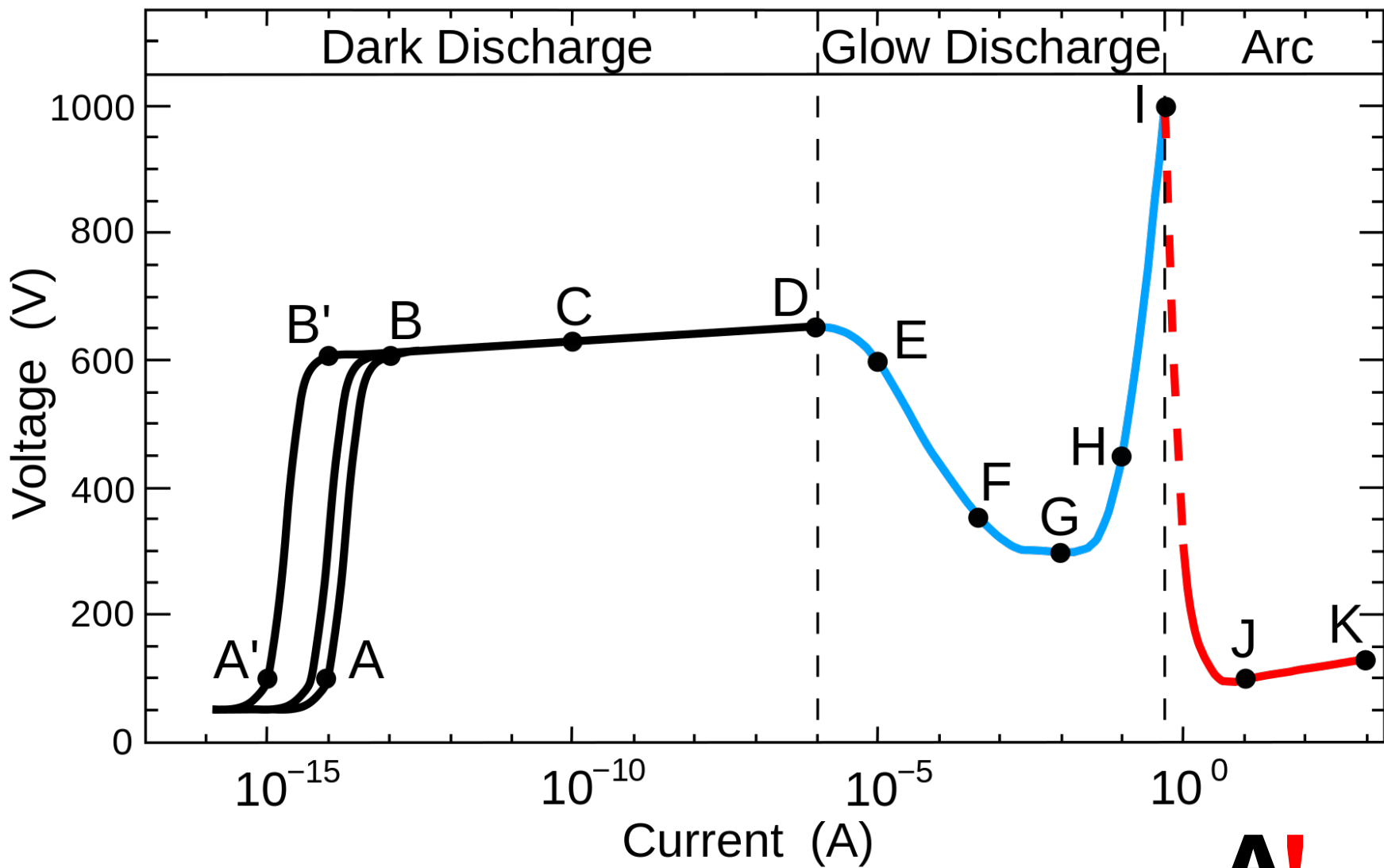
Glow discharge



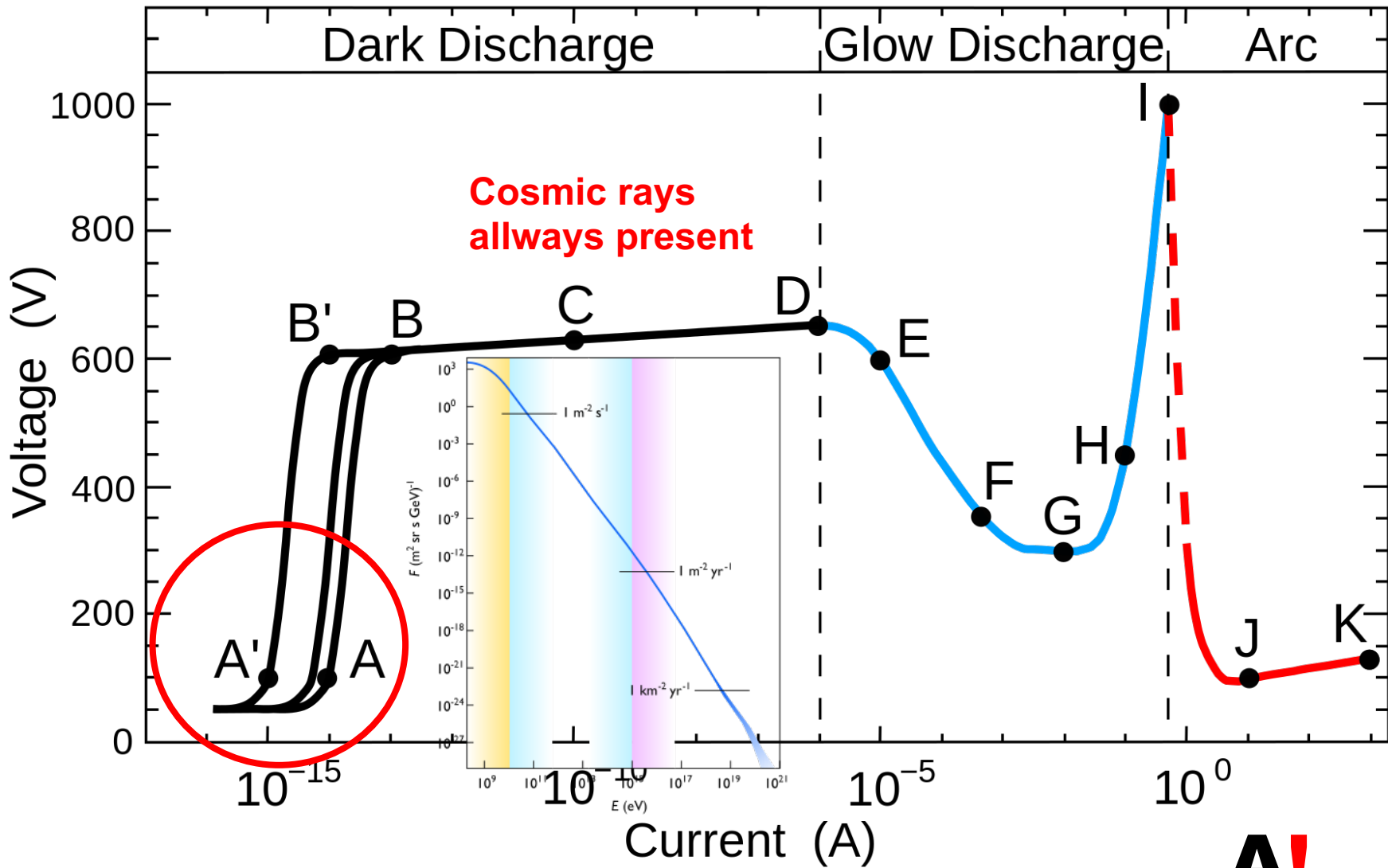
Glow discharge



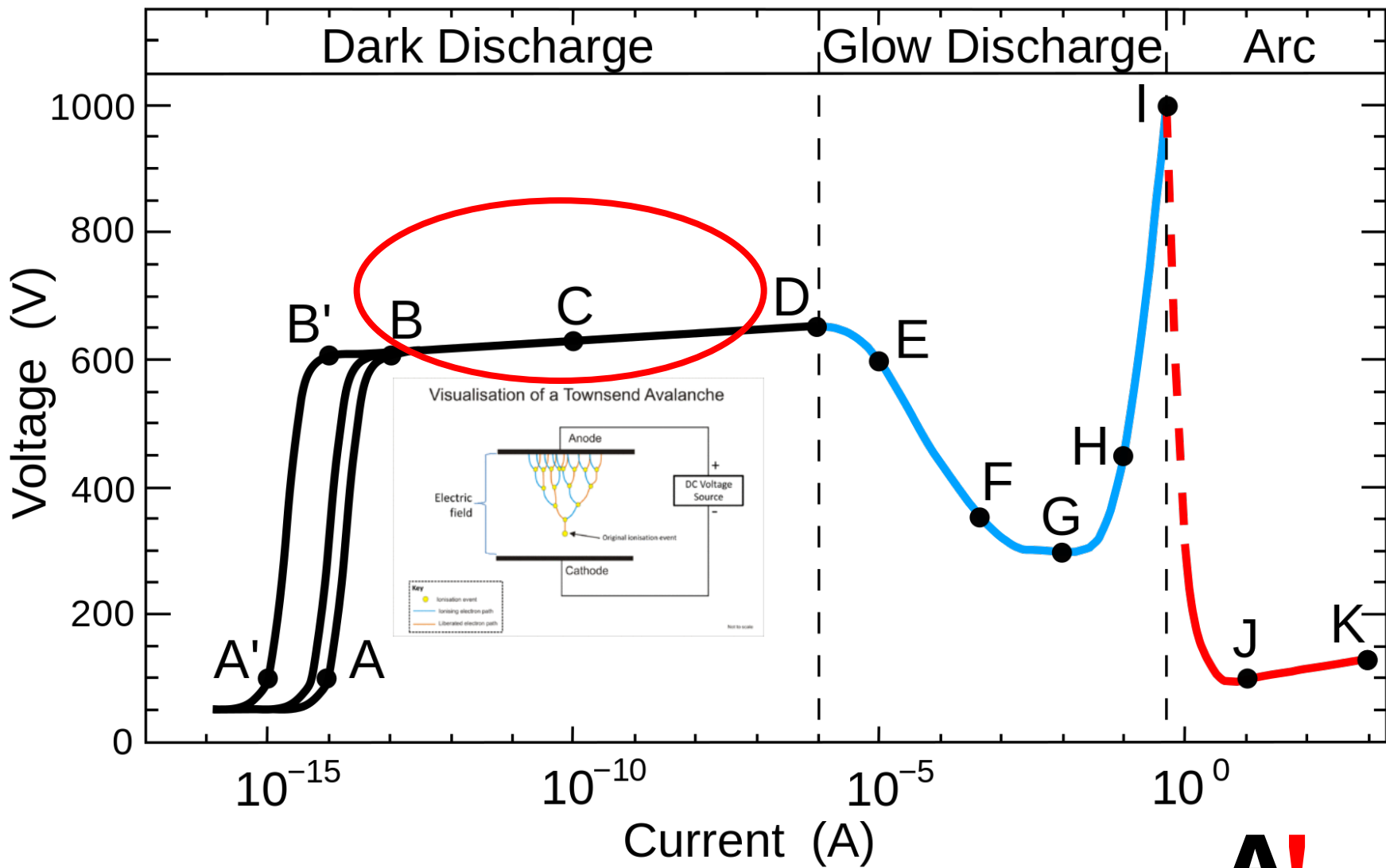
DC Plasma glow discharge and arc



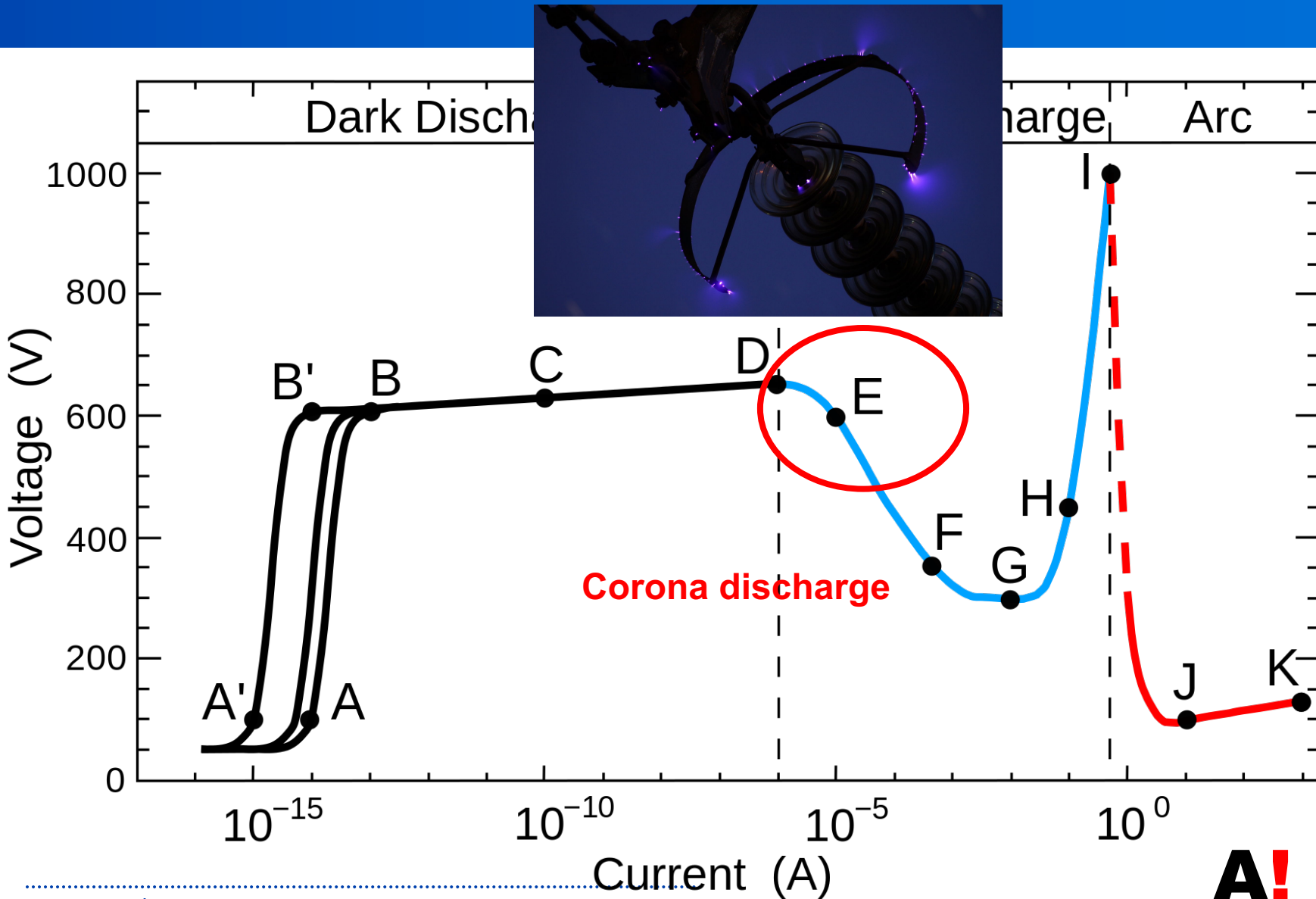
DC Plasma glow discharge and arc



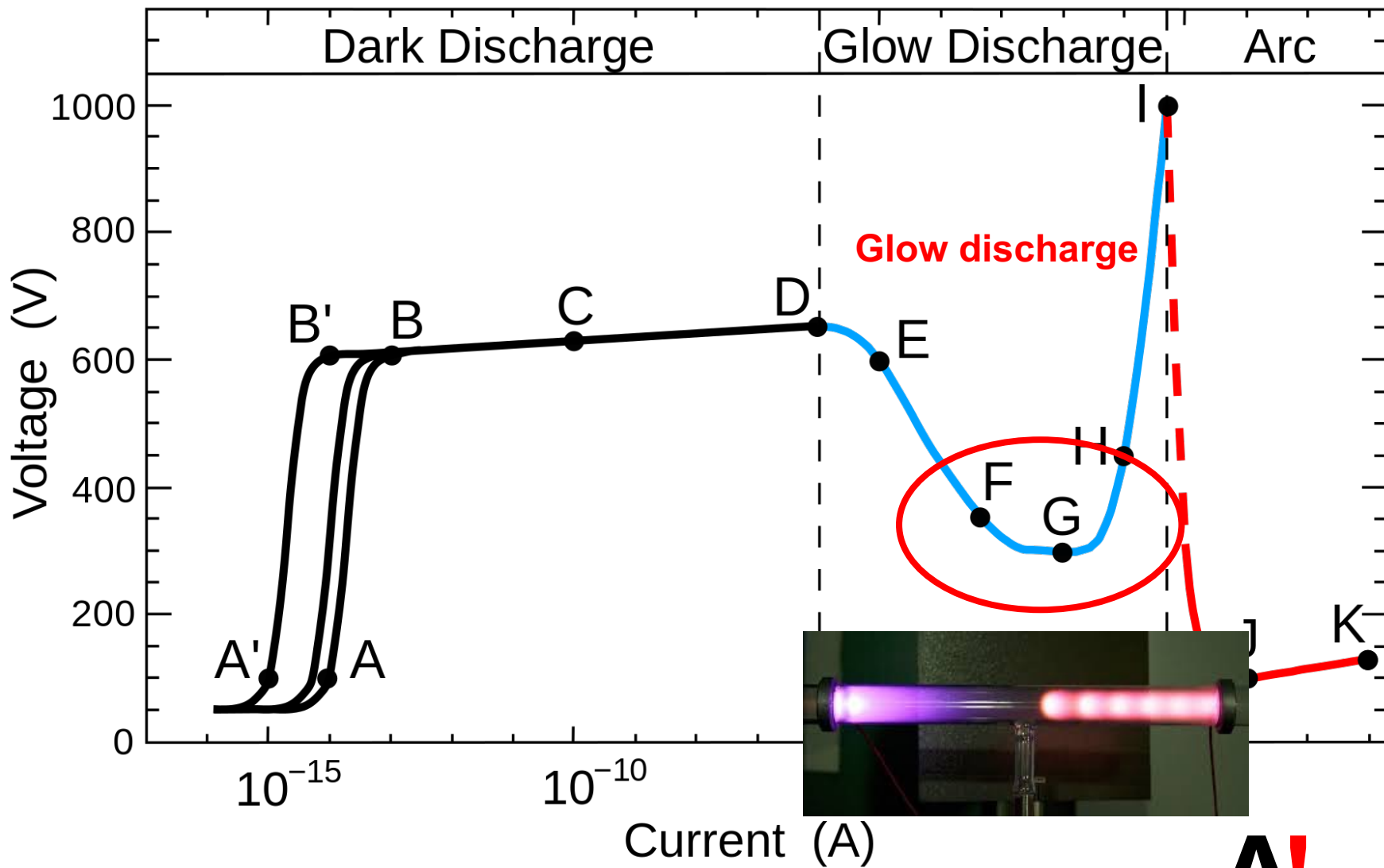
DC Plasma glow discharge and arc



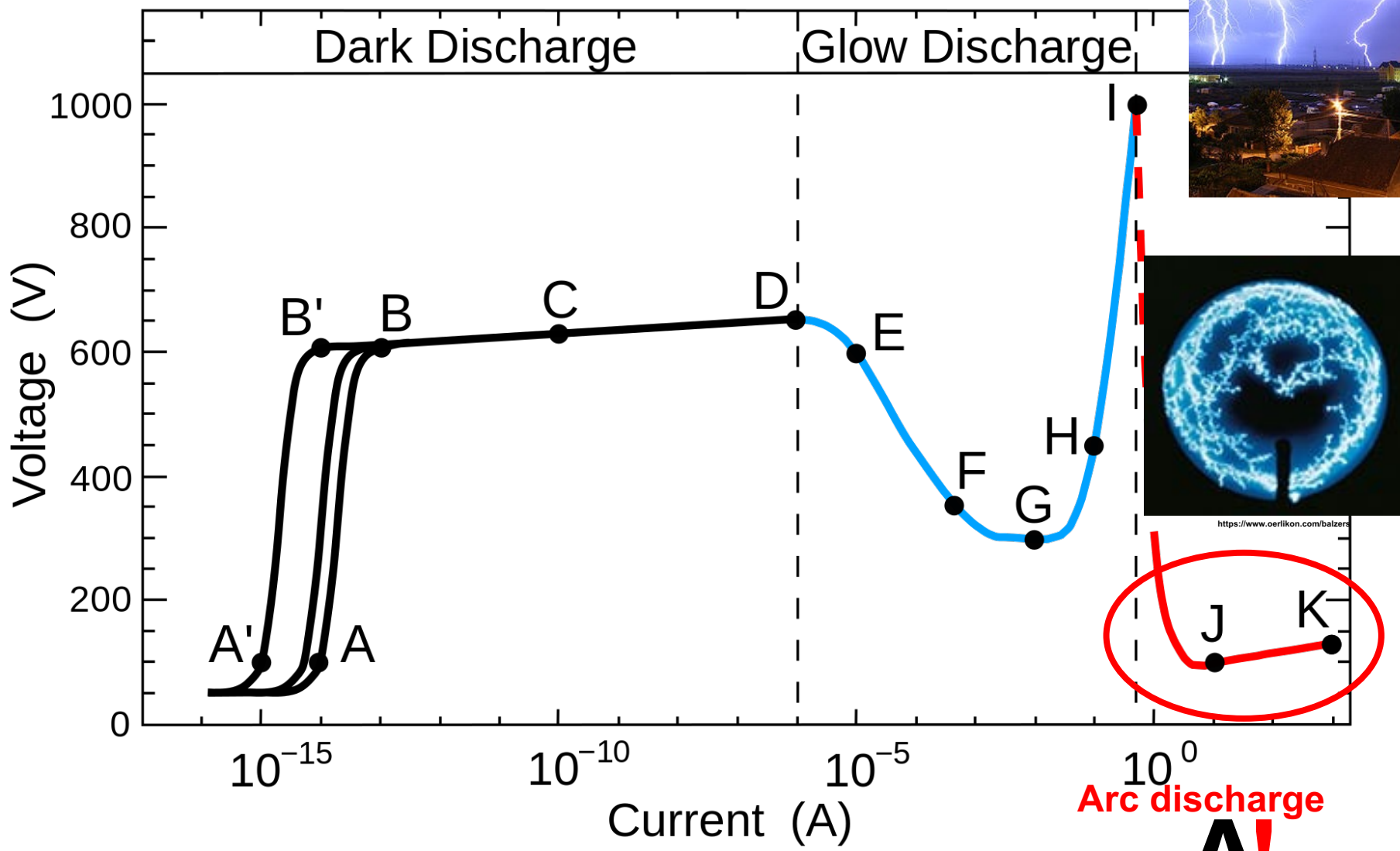
DC Plasma glow discharge and arc



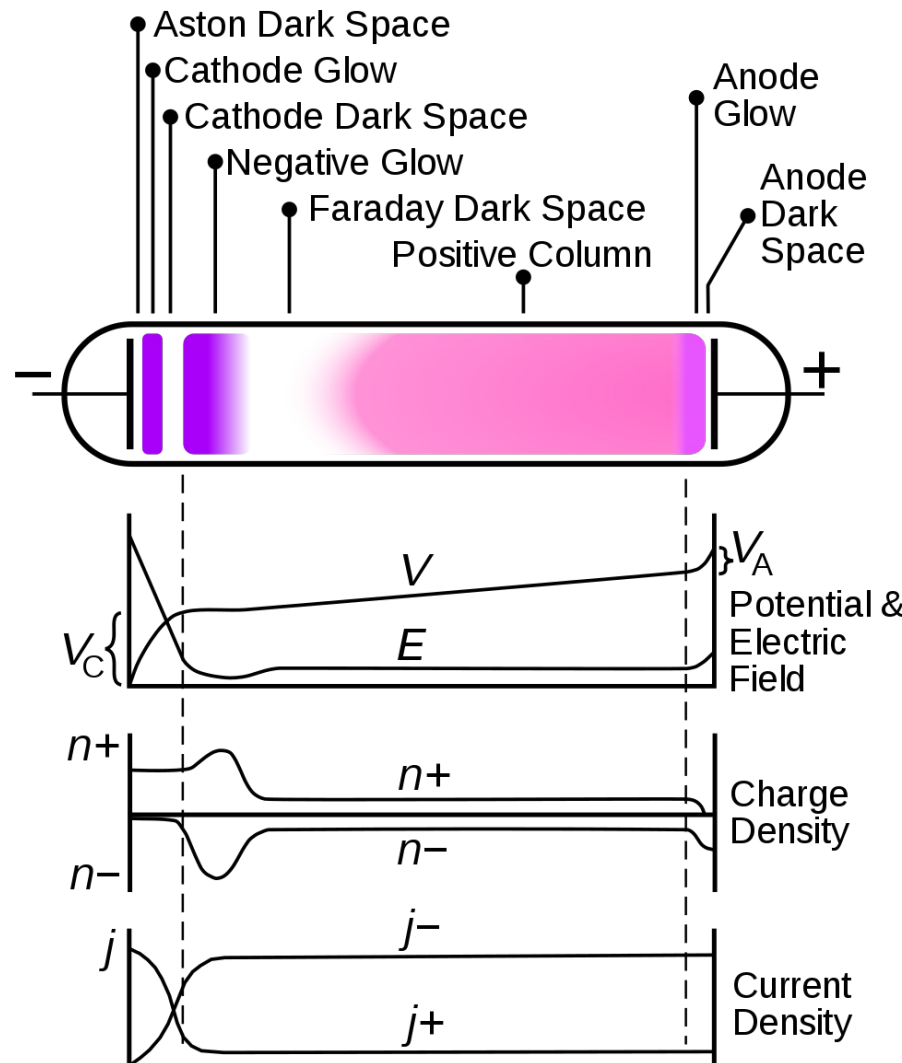
DC Plasma glow discharge and arc



DC Plasma glow discharge and arc

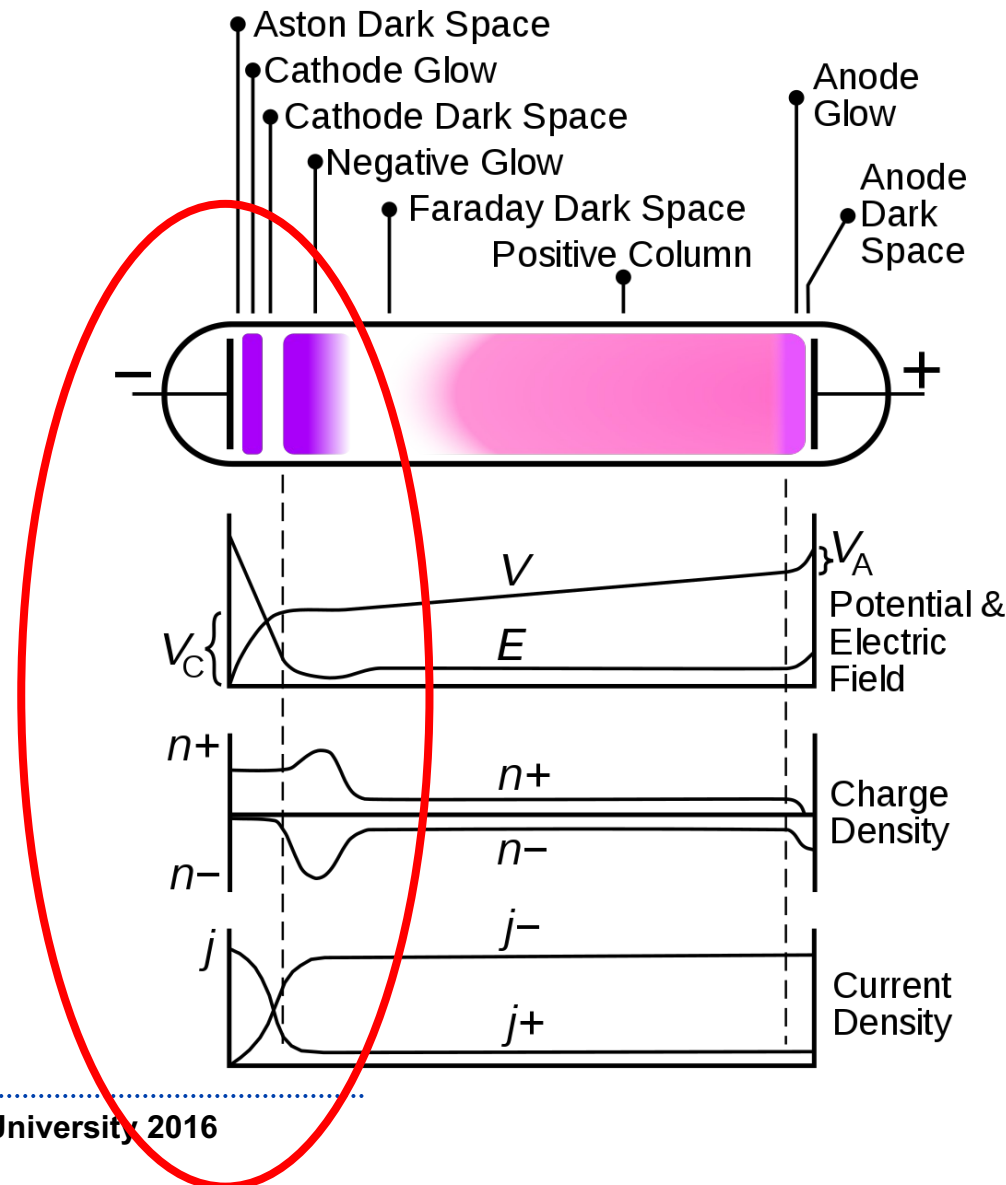


Glow discharge plasma

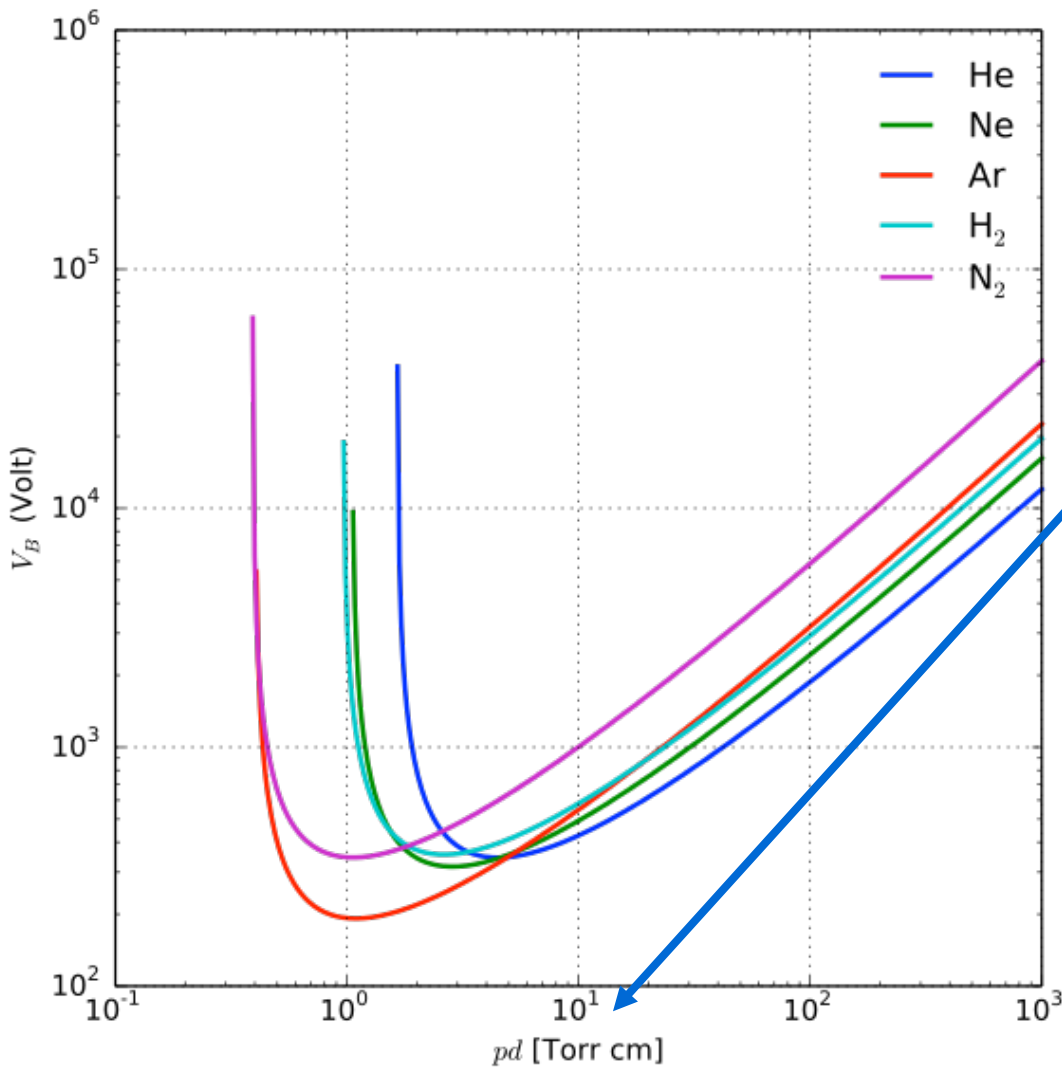


Glow discharge plasma

For PVD
Interesting things
happen
here

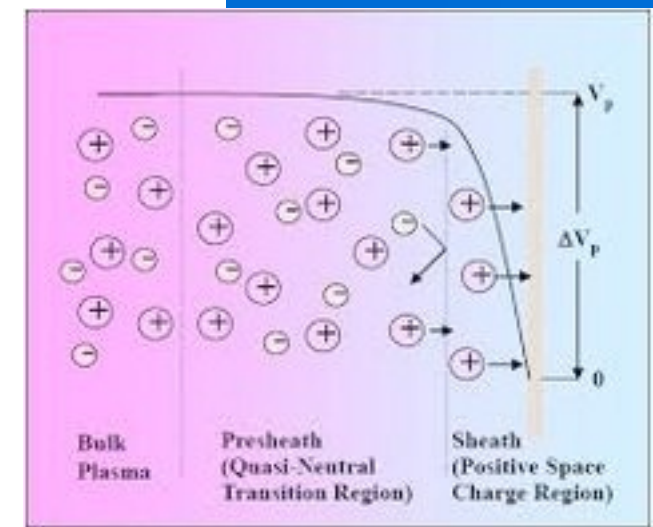
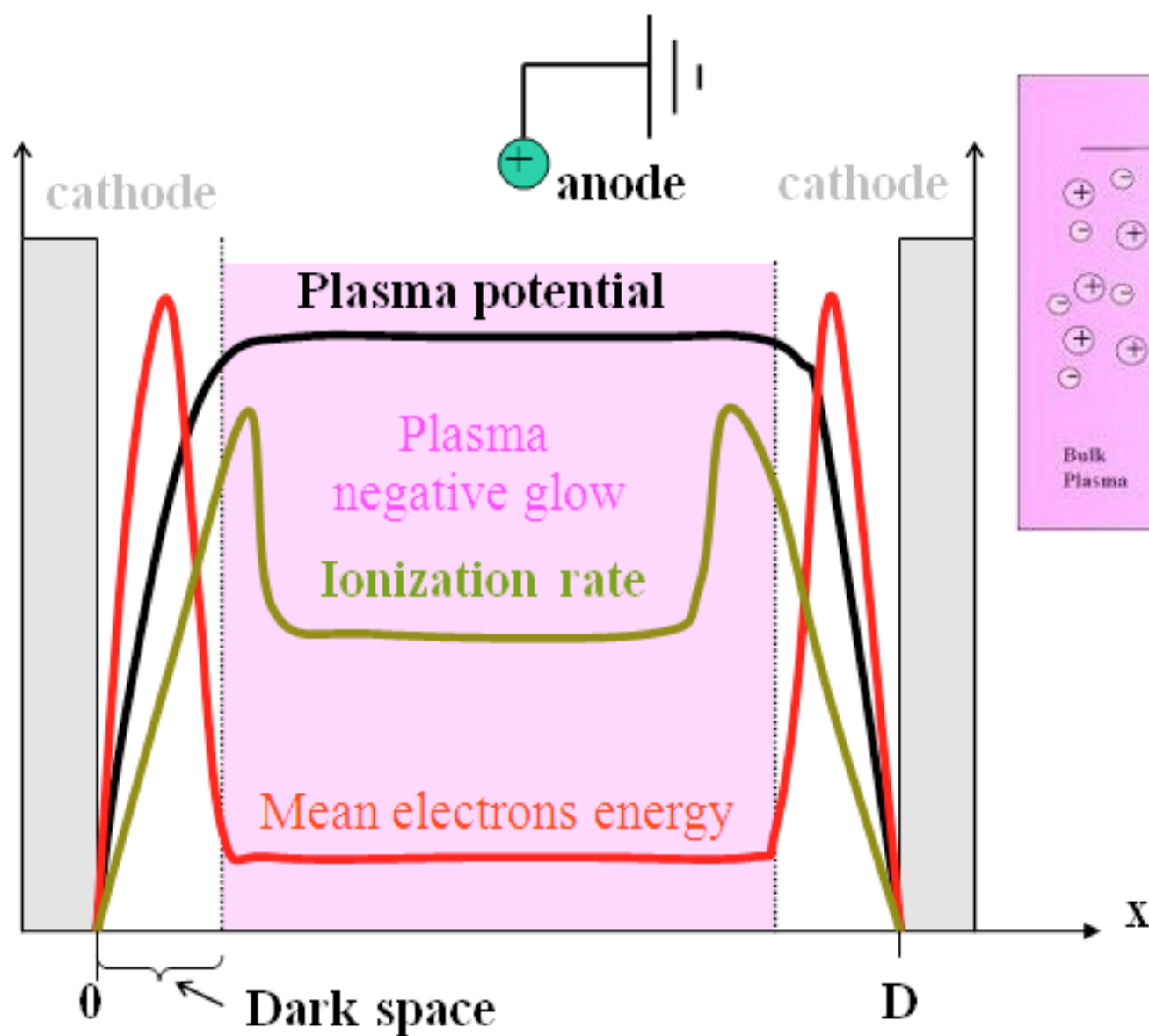


Breakdown voltage Pasheschen minimum



P pressure
d distance between electrodes

DC plasma



Important plasma parameters

- Oscillations
- Debye length
- mean free path
- ionization crossection

Plasma oscillation

Assume: n_0 fixed ions (+) & n_0 moving electrons (-)

Apply a small electric field \mathbf{E}_1 $n_+ = n_0$

→ electrons move: $n_- = n_0 + n_1(\mathbf{r}, t)$; $n_1 \ll n_0$

Electron continuity equation: $\frac{\partial n}{\partial t} + \nabla \cdot (n\mathbf{u}) = 0$

$n = n_0 + n_1(\mathbf{r}, t)$; $\mathbf{u} = \mathbf{u}_0 + \mathbf{u}_1(\mathbf{r}, t)$ ($\mathbf{u}_0 = 0 \leftrightarrow$ electrons are assumed cold)

$$\cancel{\frac{\partial n_0}{\partial t}} + \frac{\partial n_1}{\partial t} + \nabla \cdot ((n_0 + n_1)\mathbf{u}_1) = 0 \Rightarrow \frac{\partial n_1}{\partial t} + n_0 \nabla \cdot \mathbf{u}_1 + \nabla \cdot (\cancel{n_1 \mathbf{u}_1}) = 0$$

0 2nd order

Linearized continuity equation (1st order terms only): $\frac{\partial n_1}{\partial t} + n_0 \nabla \cdot \mathbf{u}_1 = 0$!!

Force: $\mathbf{F} = q\mathbf{E} \Rightarrow m_e \frac{\partial \mathbf{u}_1}{\partial t} = -e\mathbf{E}_1$

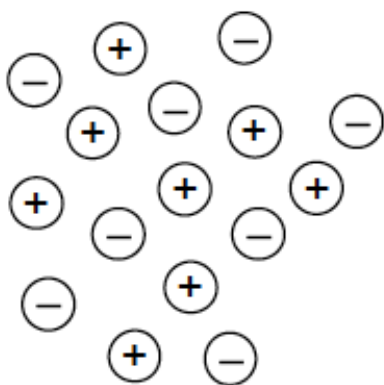
$$\Rightarrow \frac{\partial^2 n_1}{\partial t^2} + \left(\frac{n_0 e^2}{\epsilon_0 m_e} \right) n_1 = 0$$

1st Maxwell: $\nabla \cdot \mathbf{E}_1 = -en_1/\epsilon_0$

$$\omega_{pe}^2 = \frac{n_0 e^2}{\epsilon_0 m_e}$$

plasma frequency

Debye screening



Coulomb potential of each charge: $\varphi = \frac{q}{4\pi\epsilon_0 r}$

Assume thermal equilibrium (Boltzmann distribution)

$$n_\alpha(\mathbf{r}) = n_{0\alpha} \exp\left(-\frac{q_\alpha \varphi}{k_B T_\alpha}\right) \quad \alpha \text{ labels the particle populations (e.g., e, p)}$$

Introduce a test charge q_T . What will be its potential?

Home exercise: $\varphi = \frac{q_T}{4\pi\epsilon_0 r} \exp\left(-\frac{r}{\lambda_D}\right) \quad ; \quad \lambda_D^{-2} = \frac{1}{\epsilon_0} \sum_\alpha \frac{n_{0\alpha} q_\alpha^2}{k_B T_\alpha}$

Debye length: $\lambda_D \propto \sqrt{\frac{T}{n}}$

Plasma parameter: $\Lambda = n_0 \lambda_D^3 \gg 1$

Number of particles in a Debye sphere: $N = \frac{4\pi}{3} n_0 \lambda_D^3$

"Definition of plasma"

$$\frac{1}{\sqrt[3]{n_0}} \ll \lambda_D \ll L$$

L is the size of the system

Collisions

Cross section: σ (m^2) Mean free path: $l_{mfp} = 1/(n\sigma)$

Collision frequency: $\nu_c = n\sigma v$

Hannu Koskinen Univ of Helsinki

n = density of atoms (and ions)

Total collision cross section:

$$\sigma_{\text{total}} = \sigma_{\text{excitation}} + \sigma_{\text{ion}} + \sigma_{\text{attachment}} + \sigma_{\text{other}}$$

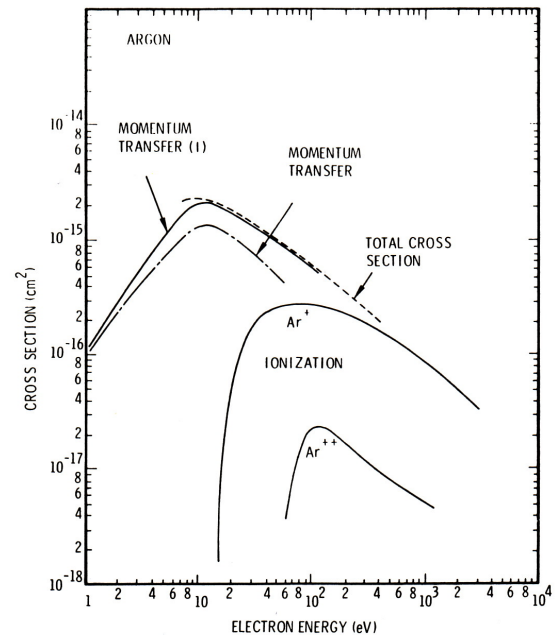
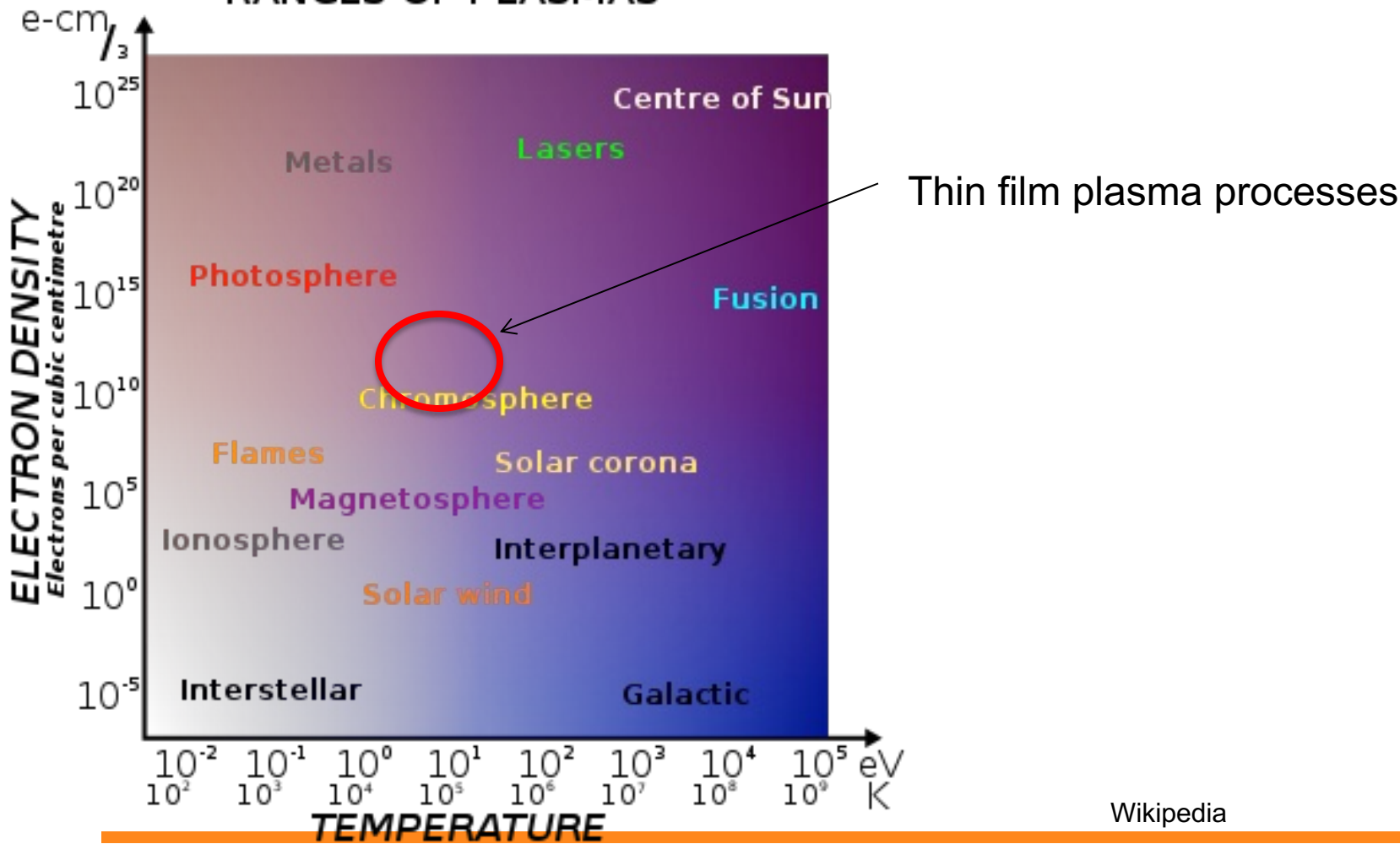


Figure 2.1. Collision cross sections for electrons in Ar gas (from Ref. 1).

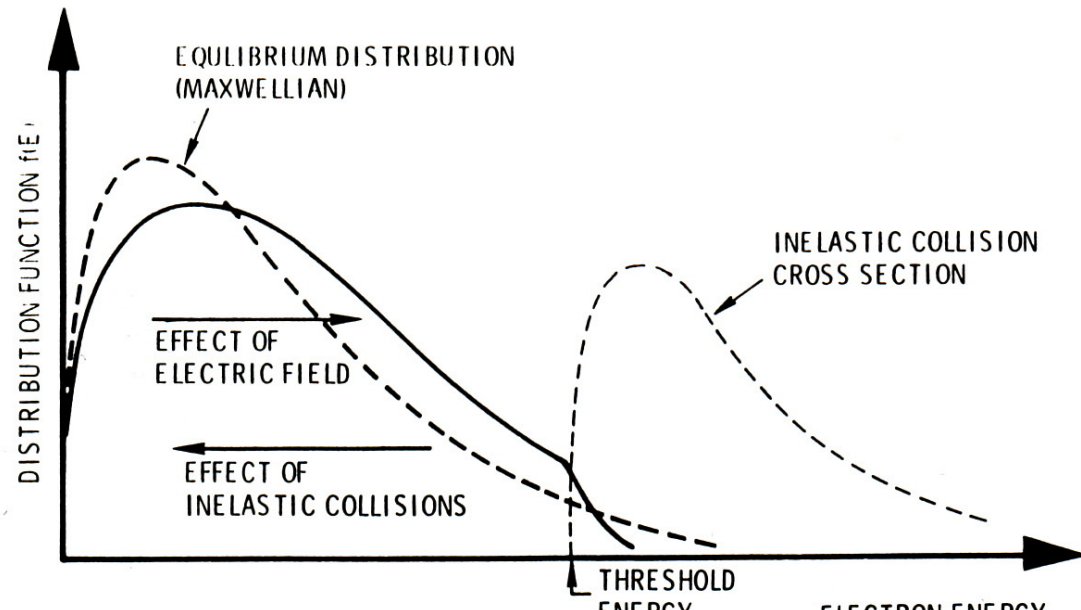
Bunshah, Handbook of Deposition Technologies for Films and Coatings Noyes

Different types of plasmas

RANGES OF PLASMAS



Electron temperature



Bunshah, "Handbook of Deposition Technologies for Films and Coatings Noyes

A

Figure 2.4. Schematic illustration of electron energy distribution function and inelastic collision cross section.

Electron and ion temperature

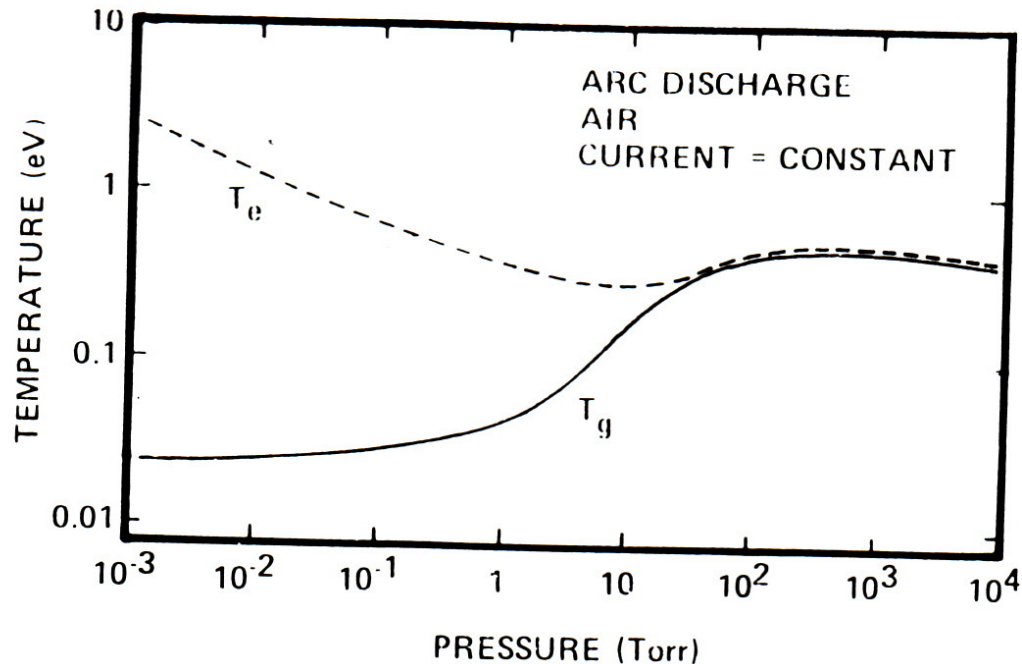


Figure 2.3. Electron (T_e) and gas temperatures (T_g) in an air arc as a function of pressure (from Ref. 5).

Bunshah, Handbook of Deposition Technologies for Films and Coatings Noyes

Plasma sheath

Sheath thickness $d_s \sim \text{constant}^* \lambda_D$
constant $\approx 5 - 40$
Glow discharge $d_s \approx 0.15 - 2 \text{ mm}$

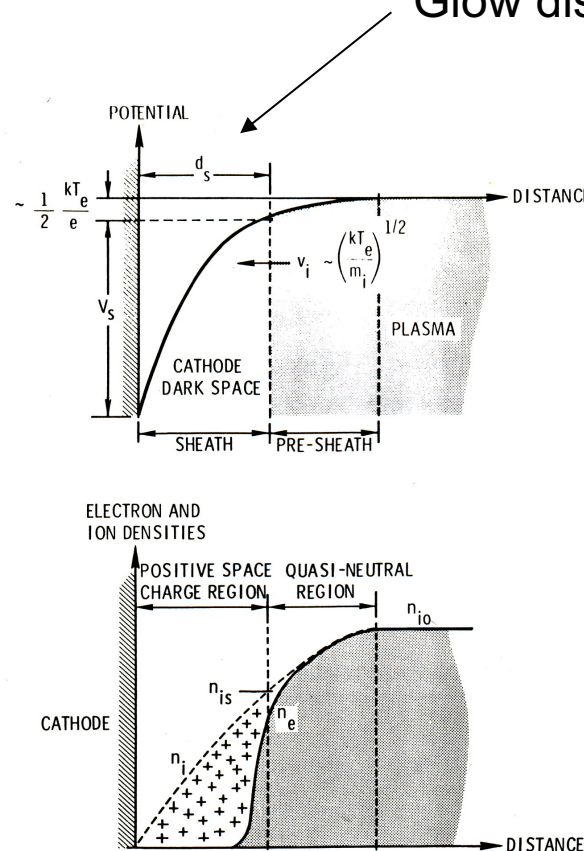


Figure 2.9. Schematic representation of the positive space-charge sheath that develops over a cathode (from Ref. 1).

Bunshah, Handbook of Deposition Technologies for Films and Coatings Noyes

Cold cathode discharge

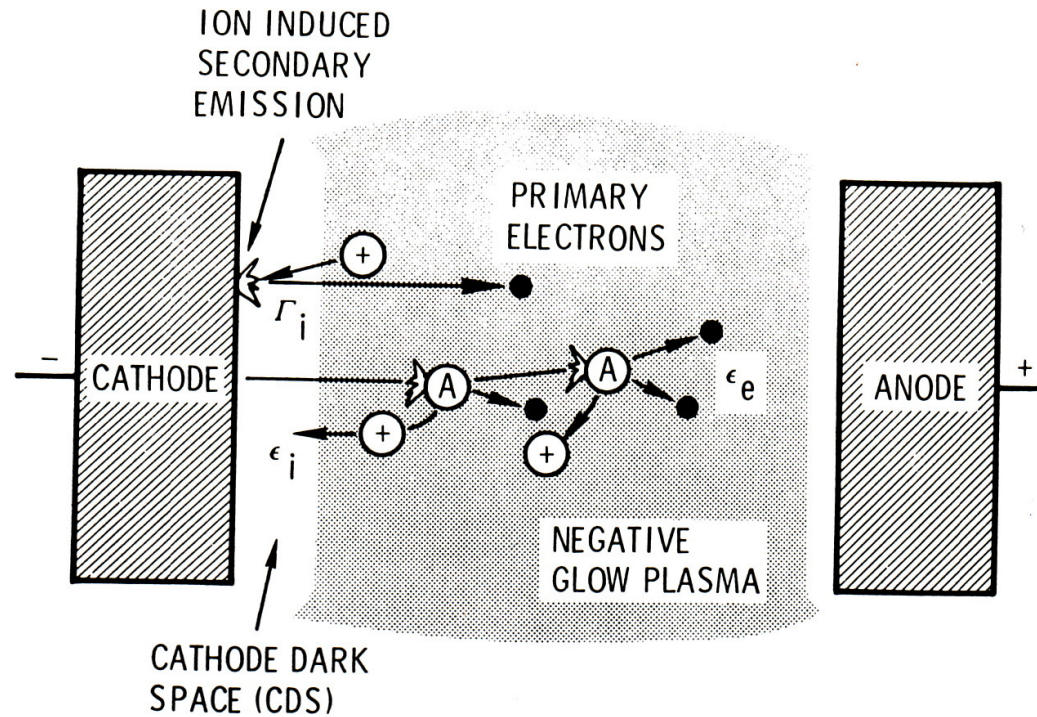
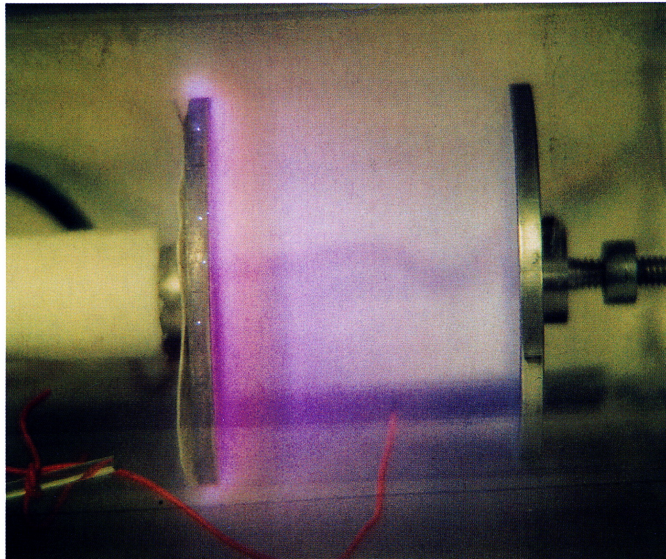


Figure 2.18. Schematic illustration of a cold-cathode discharge.

Bunshah, Handbook of Deposition Technologies for Films and Coatings Noyes

Luminous regions in DC plasma



Colorplate VI.18 A DC glow discharge in argon. The anode (grounded) is on the right and the cathode (supported by a white teflon insulator) on the left. The orange wire is a Langmuir probe whose bare tip enters the positive column of the discharge. The positive column is the largest luminous region, which extends about 75% of the way from the anode toward the cathode. The pressure was 100 mtorr and the voltage applied between cathode and anode was 1 kV. The discharge current density was 0.22 mA/cm².

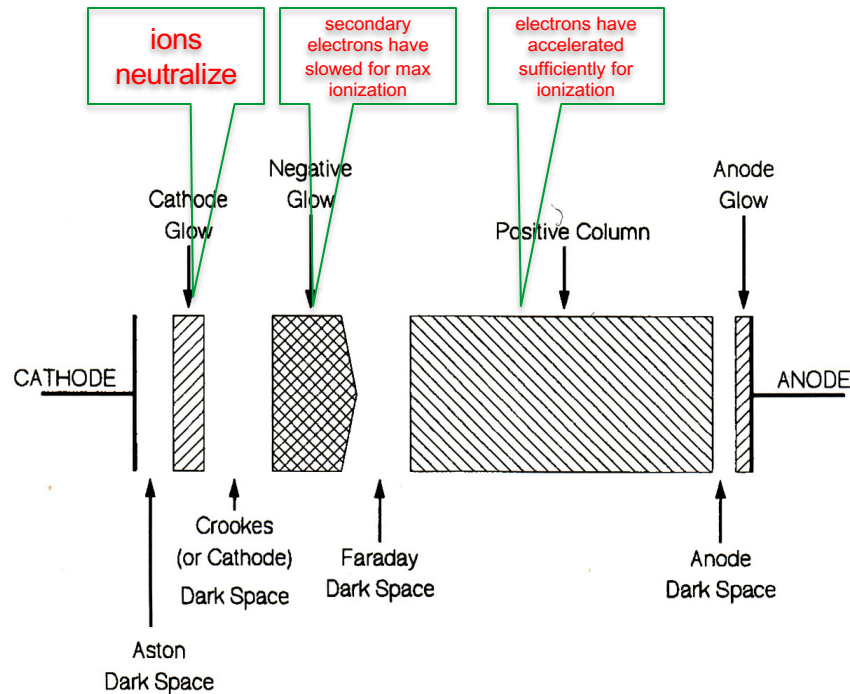


Figure VI.17 The classical luminous and dark regions of a DC glow discharge, based on classifications by early researchers [Holland, 1956; Maissel and Glang, 1970; Brown, 1966; Nasser, 1971, Llewellyn-Jones, 1966; Cobine, 1941; von Engel, 1965].

Practical sputtering plasma -1

- Argon pressure 1 torr
- atom density (n) $3 \times 10^{16} \text{ cm}^{-3}$
- $n_i = n_e$ 10^{10} cm^{-3}
- ionization fraction 3×10^{-7} (weakly ionized plasma)
- ion temperature T_i 300K
- electron temperature T_e 23,000K

Practical sputtering plasma -2

- V_{DC} 1000V
- V_p 8V
- Current density at cathode 2 mA/cm²
- Cathode sheath L 2 mm
- mean free path λ 50 μm

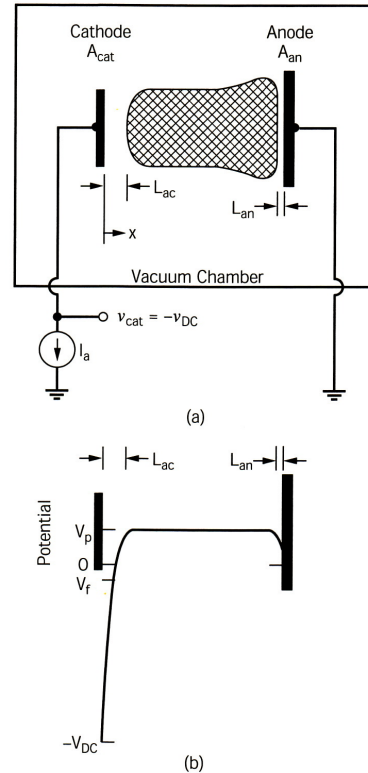


Figure VI.8 (a) Schematic diagram of a DC sputtering discharge; (b) the potential profile (not to scale, as $V_p - V_f$ is typically much less than V_{DC}).

Mahan, Physical Vapor Deposition of Thin Films, Wiley

Circuit models of DC plasma discharge

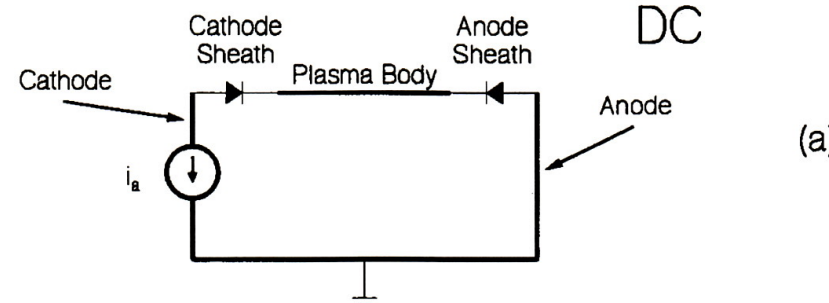
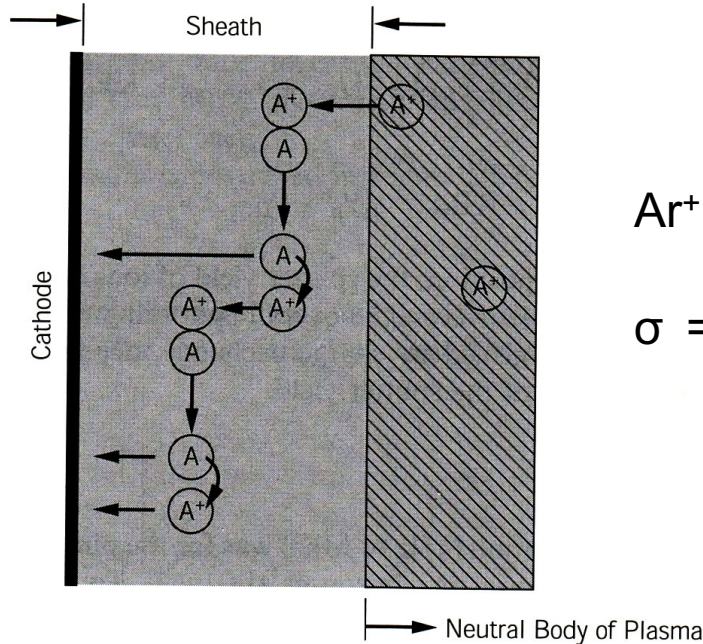


Figure VI.9 Circuit models for (a) a DC sputtering discharge and (b) a capacitive RF sputtering discharge.

Mahan, Physical Vapor Deposition of Thin Films, Wiley

Ion energy at cathode



$$\sigma = 2.5 \times 10^{-15} \text{ cm}^{-3}$$

Figure VI.10 The process of symmetric charge exchange within the cathode sheath. When two charge exchange events occur, as shown here, a single ion entering the sheath is converted into two neutrals plus an ion, all of which strike the cathode (but with kinetic energies corresponding to only a fraction of the cathode fall).

Mahan, Physical Vapor Deposition of Thin Films, Wiley

AC plasma methods

AC plasma

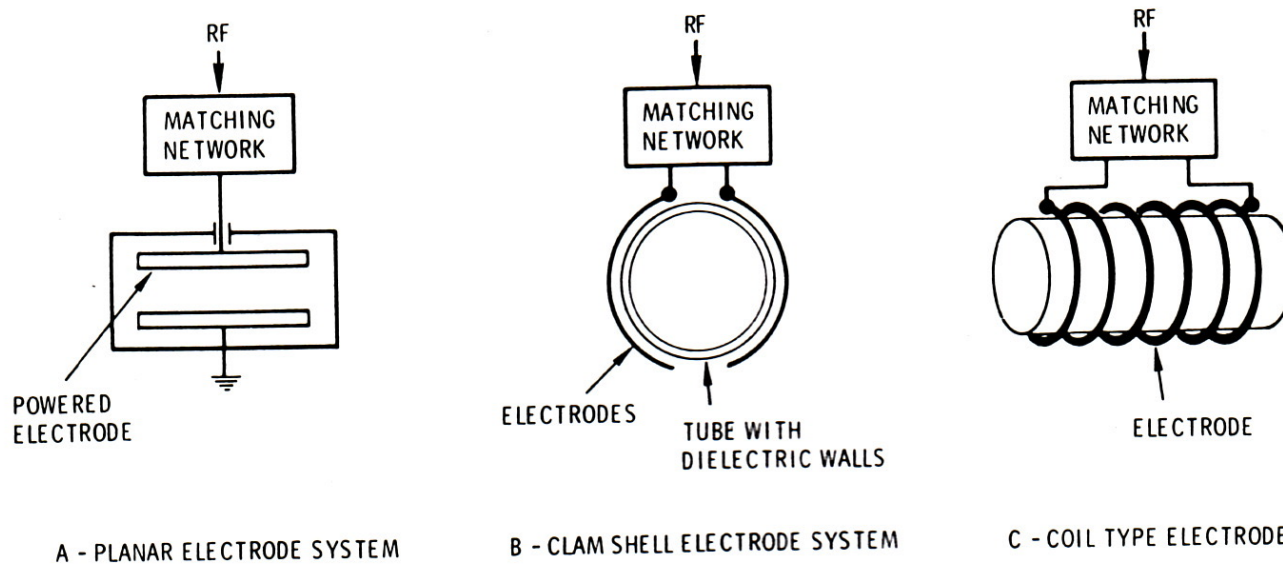


Figure 2.12. Schematic illustration of glow discharge devices commonly used in plasma-assisted materials processing.

Bunshah, Handbook of Deposition Technologies for Films and Coatings Noyes

Forming of self-bias in AC discharge

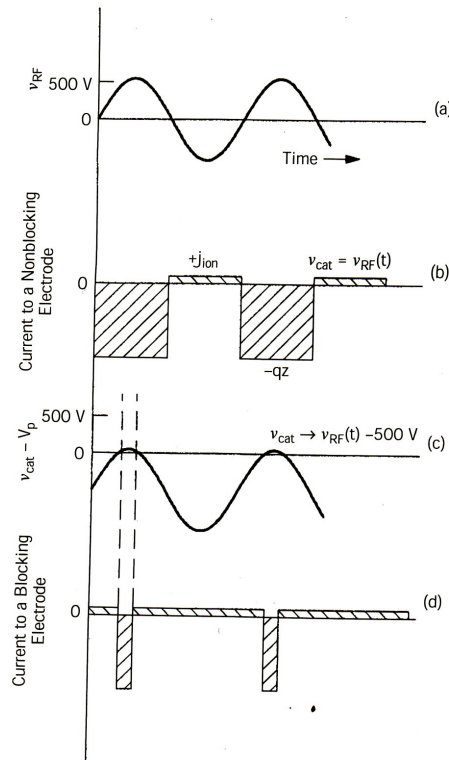
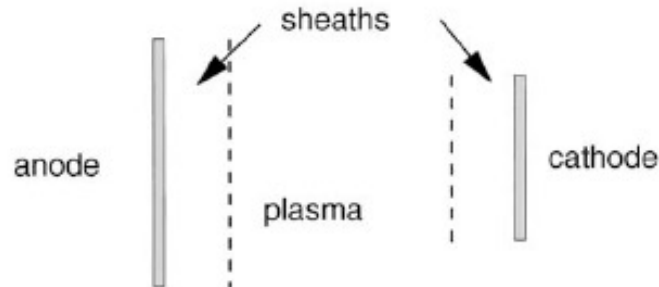


Figure VI.11 DC self-bias. Potentials and currents for RF excitation of (a–b) nonblocking and (c–d) blocking electrodes.

Mahan, Physical Vapor Deposition of Thin Films, Wiley

Self bias at electrodes

$$\frac{V_1}{V_2} = \left(\frac{A_2}{A_1} \right)^n$$



$n= 4$ (sometimes 2)

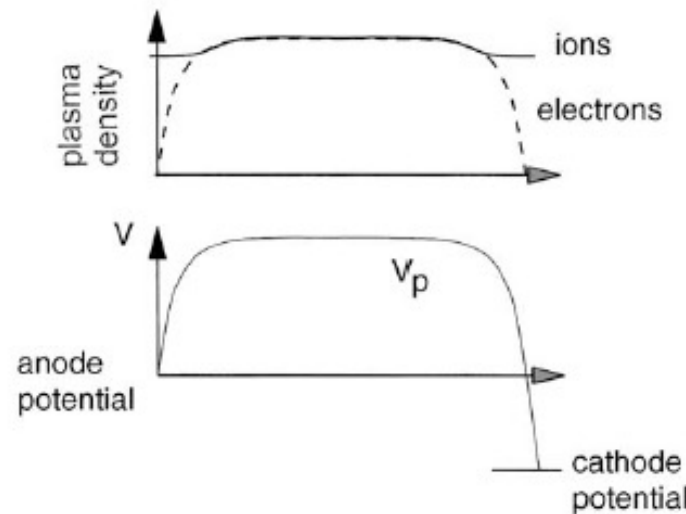


Fig. 7. Electron and ion distributions which create sheaths between the neutral plasma and the walls.

Circuit models of RF plasma discharge

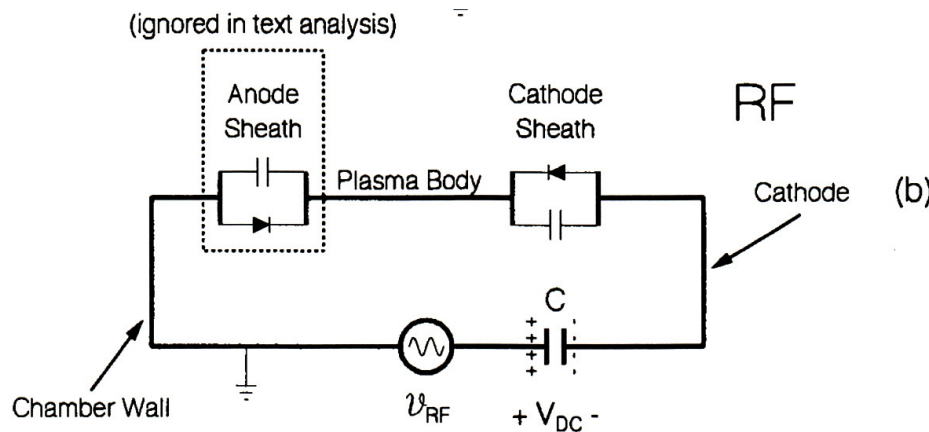
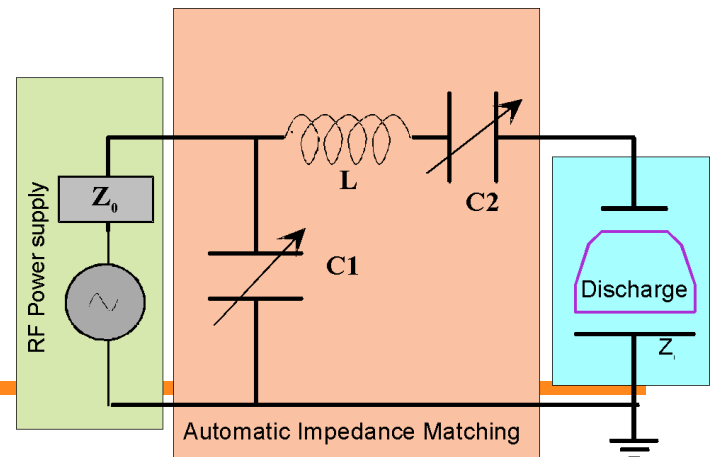
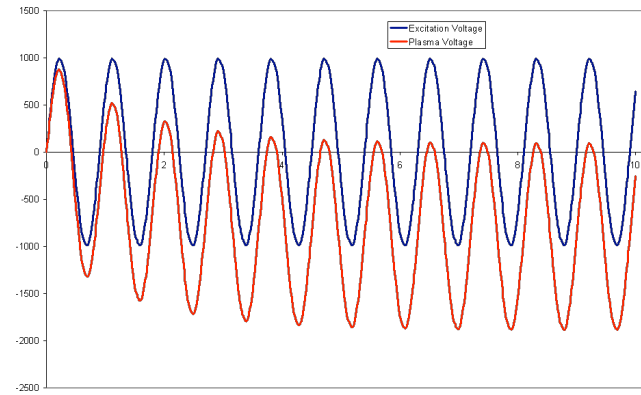
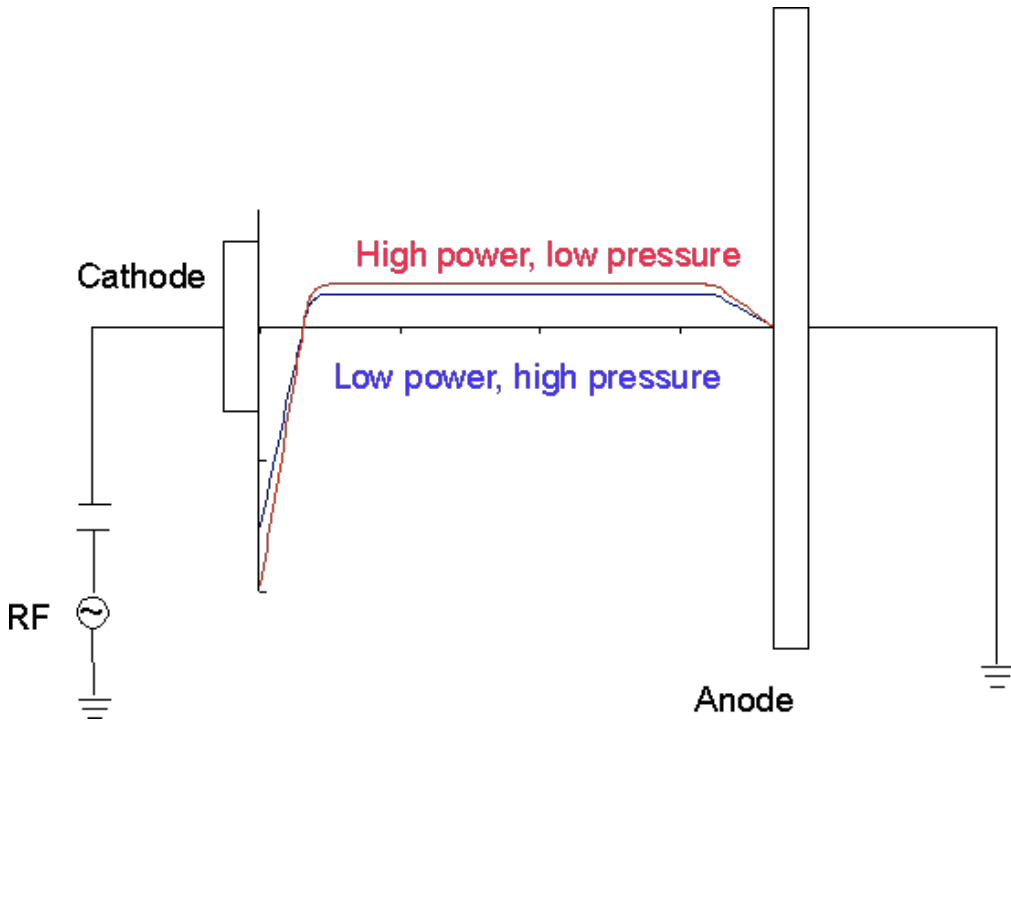


Figure VI.9 Circuit models for (a) a DC sputtering discharge and (b) a capacitive RF sputtering discharge.

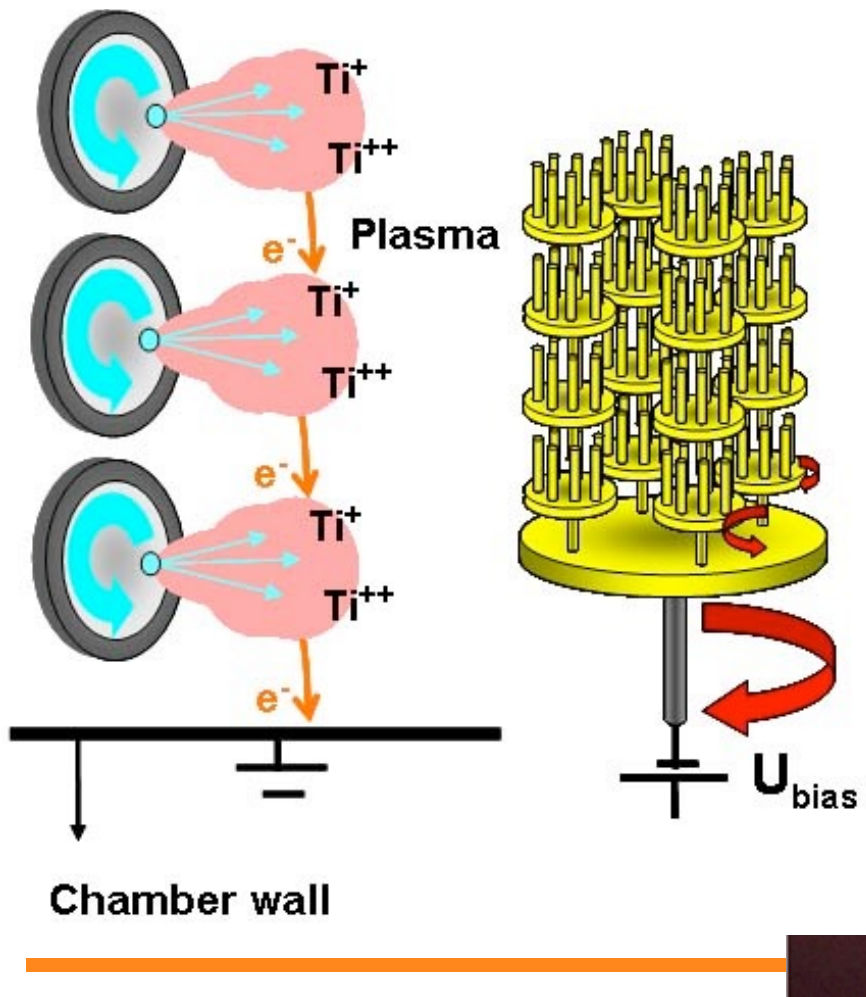
Mahan, Physical Vapor Deposition of Thin Films, Wiley

RF Plasma glow discharge



Arc plasma

Arc discharge deposition



Particles in cathodic arc

<https://www.youtube.com/watch?v=gM86v350HhM&t=60s>

Cathodic arc spot evolution

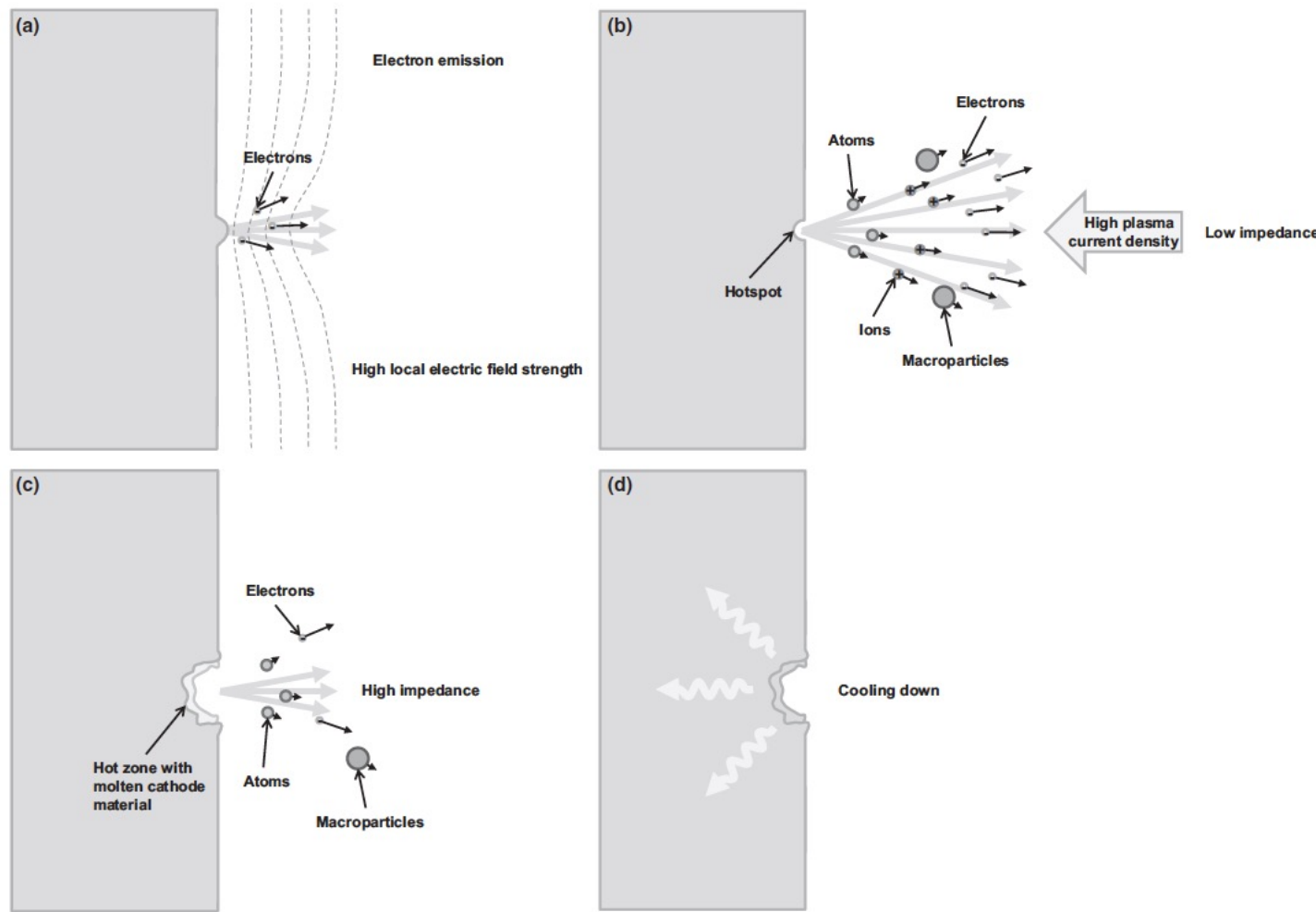
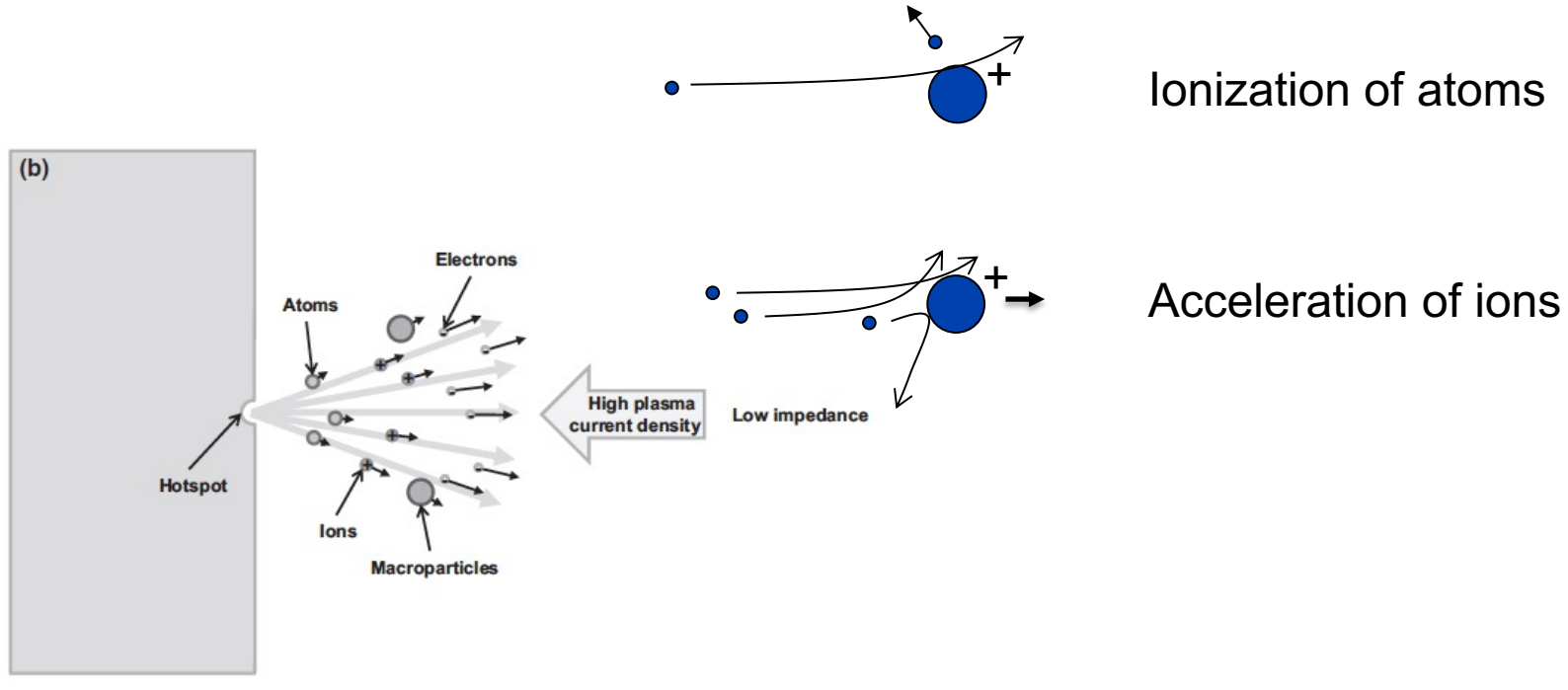


Figure 13 The evolution of the cathode spot in four stages. (a) Pre-explosion; (b) explosive stage; (c) cooling with molten cathode material; and (d) final cooling.

Koskinen, J. Cathodic-Arc and Thermal-Evaporation Deposition. In Comprehensive Materials Processing; Cameron, D., Ed.; Vol. 4; Elsevier Ltd., 2014, 2014; pp 3–55. ISBN: 9780080965321

Electron wind causes ionization and acceleration of atoms

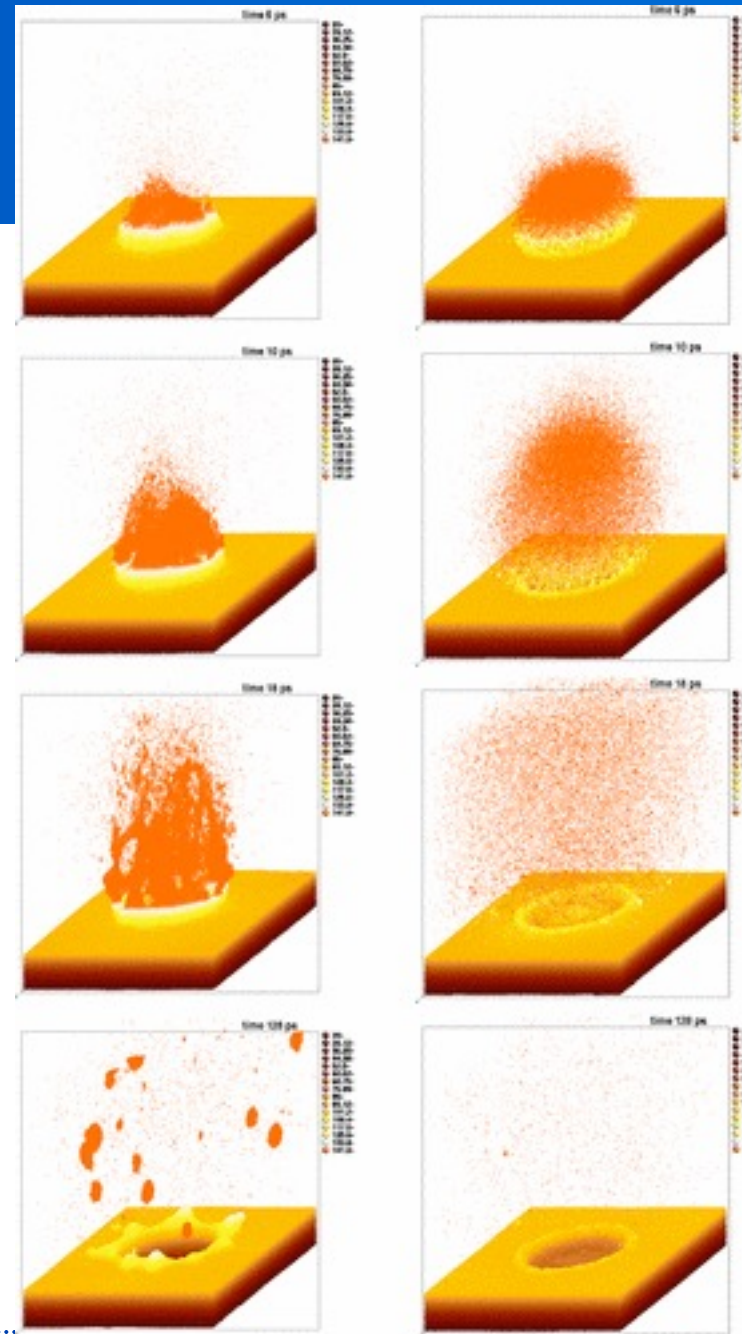


Koskinen, J. Cathodic-Arc and Thermal-Evaporation Deposition. In Comprehensive Materials Processing; Cameron, D., Ed.; Vol. 4; Elsevier Ltd., 2014, 2014; pp 3–55. ISBN: 9780080965321

Arc spot evolution by numeric simulation

Left:
energetic
plasma ion
flux

Right: local
thermal
heating



Cu atoms, Cu⁺ ions and electrons near cathode spot by numerical simulations

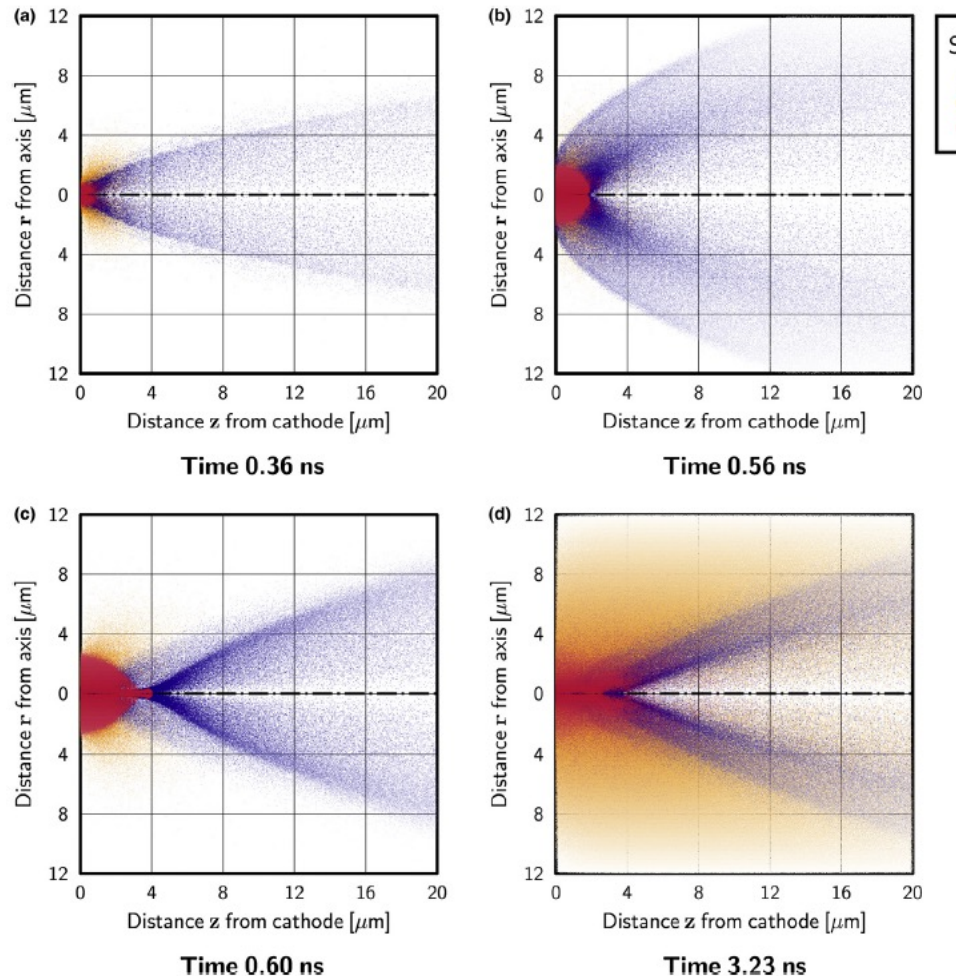


Figure 14 Time evolution of the plasma initiation process in four time steps obtained by numerical modeling. Reproduced from Timko, H. Modelling Vacuum Arcs: From Plasma Initiation to Surface Interactions. Report Series in Physics HU-P-D188, Theses, 2011.

Koskinen, J. Cathodic-Arc and Thermal-Evaporation Deposition. In Comprehensive Materials Processing; Cameron, D., Ed.; Vol. 4; Elsevier Ltd., 2014, 2014; pp 3–55. ISBN: 9780080965321

Cathodic arc spot evolution

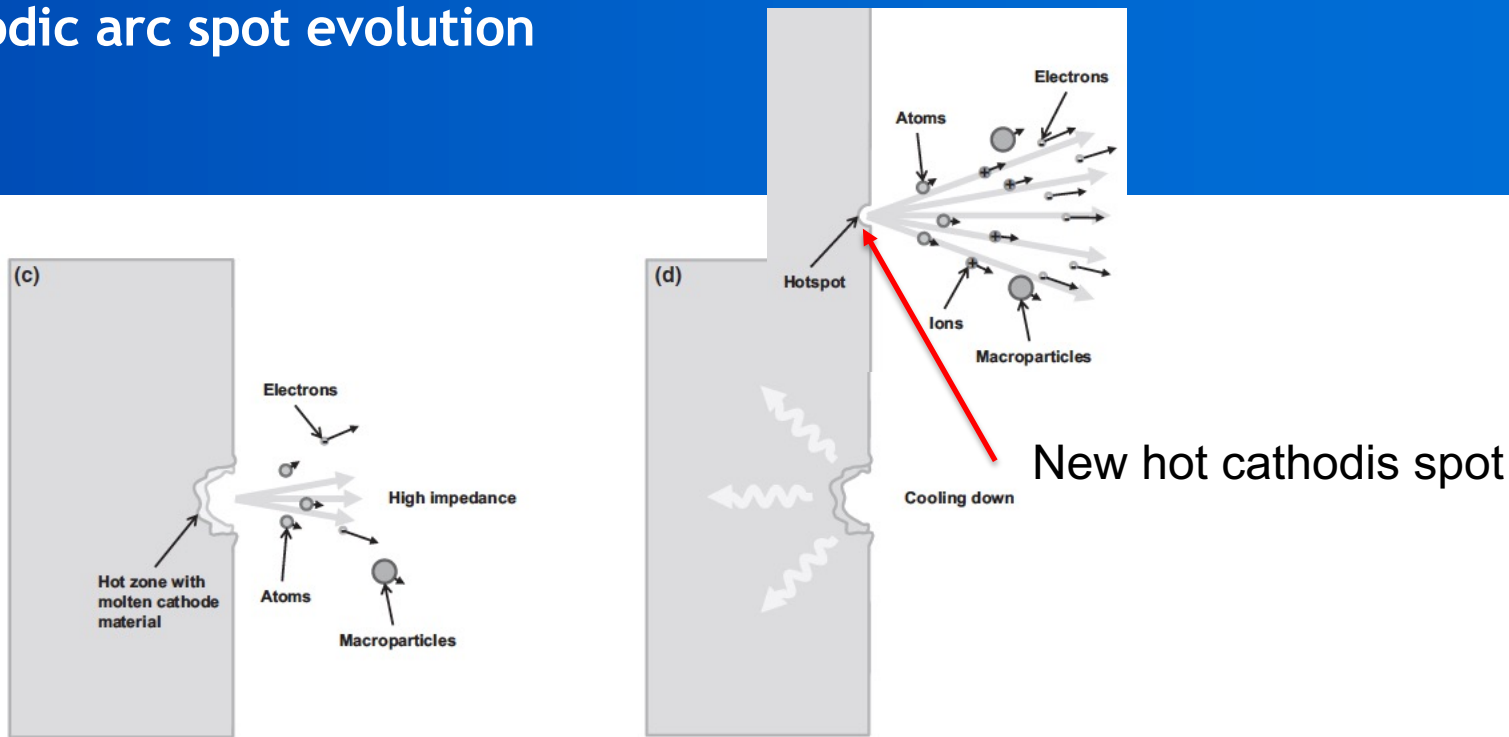
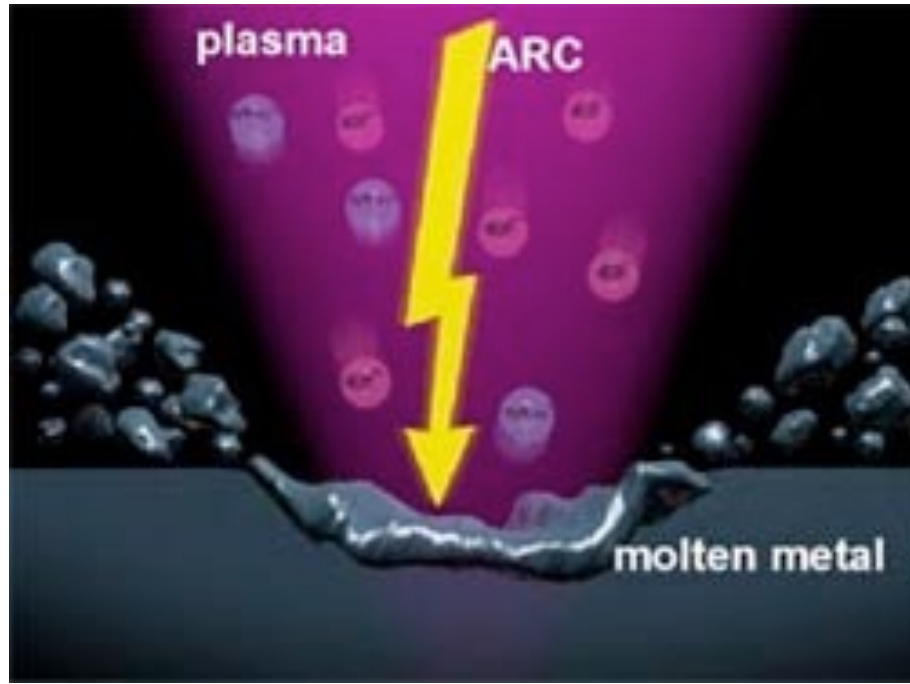


Figure 13 The evolution of the cathode spot in four stages. (a) Pre-explosion; (b) explosive stage; (c) cooling with molten cathode material; and (d) final cooling.

Koskinen, J. Cathodic-Arc and Thermal-Evaporation Deposition. In Comprehensive Materials Processing; Cameron, D., Ed.; Vol. 4; Elsevier Ltd., 2014, 2014; pp 3–55. ISBN: 9780080965321

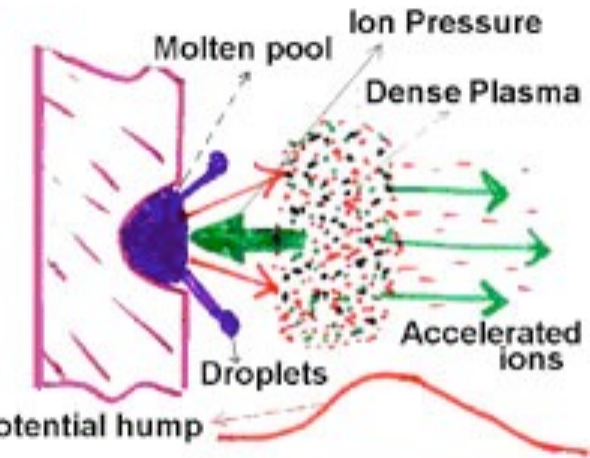
Arc discharge – cathode spot



www.shm-cz.cz/files/schema01.jpg

Arc discharge process

- arc current concentrated into filaments – arcs
- intense electron emission
- intense ion emission due to electron current (atoms/electrons – 1/100)
- ionization of atoms – formation of plasma
- flow of ions to cathode – intense sputtering of atoms
- $10^6 - 10^8 \text{ A/m}^2$
- overlapping thermal spikes
- materials is melted and sublimated in cathode spots
- cathode spots move randomly or could be steered by using magnets
- electrons ionize vapor and create more electrons – increase of current
- ions accelerate
 - due to potential difference in plasma
 - due to multiple collisions with fast electrons
- macro particles (up to $10 \mu\text{m}$ diam.) are formed



Timko, Nordlund
simulations

<http://prb.aps.org/supplemental/PRB/v81/i18/e184109>

Filtered arc

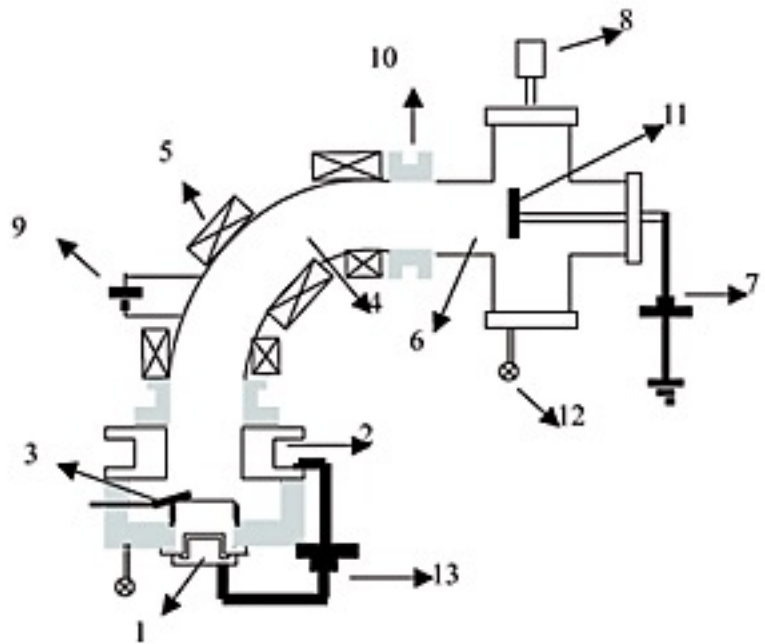
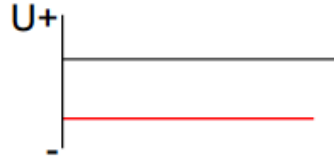


Figure 1. Scheme of the DCF2 device. (1) cathode; (2) anode; (3) trigger; (4) quarter torus magnetic filter; (5) torus coil; (6) deposition chamber; (7) probe bias source; (8) diagnostic port; (9) filter bias source; (10) insulators; (11) collecting probe; (12) vacuum pumping systems; (13) arc source.

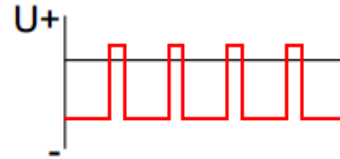
PULSED SPUTTERING

Definitions

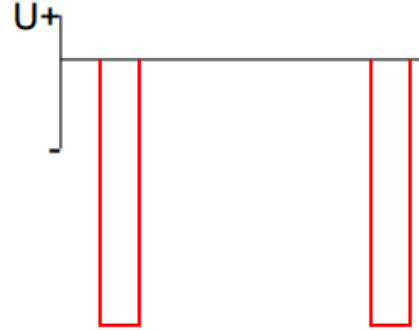
- DC-sputtering



- Pulsed DC



- HiPIMS



HIPIMS

High Power Pulsed Magnetron Sputtering (HIPIMS)

- Introduced by Kouznetsov et al.*
 - Also known as HIPIMS – High Power Impulse Magnetron Sputtering
- High power pulses of short duration
 - Peak value typically 100 times greater than conventional magnetron sputtering
 - Peak power densities of 1-3 kW/cm²
 - Pulse width of 100 - 150 µsec
 - Discharge voltages of 500-1000 V



*V. Kouznetsov, K. Macák, J. M. Schneider, U. Helmersson, and I. Petrov, "A New Sputter Technique Utilizing Very High Target Power Densities," Surf. Coat. Tec.

HIPIMS

- High degree of target material ionization
 - High secondary electron current
 - Promotes ionization of sputtered species
 - Can approach 100%, vs. up to ~10% for conventional sputtering
- Potential is to use the ions to improve film properties and structure of coatings
 - With bias can produce dense films and coat irregular shapes
 - With high ion flux and low bias voltage should be possible to deposit low stress thick films

Loss of Deposition Rate*

| Power, kW | Al Rate, nm min ⁻¹ | | Ratio, HPPMS to DC |
|--------------|-------------------------------|--------------|--------------------------|
| | HPPMS | Pulsed DC | |
| 1.0 | 22 | 70 | 0.31 |
| 2.0 | 37 | 149 | 0.25 |

- **HIPIMS** rate loss partially due to ionized sputtered species being attracted back to the target

*W. D. Sproul, D. J. Christie, and D. C. Carter, "The Reactive Sputter Deposition of Aluminum Oxide Coatings Using High Power Pulsed Magnetron Sputtering (HPPMS)," Society of Vacuum Coaters, 47th Annual Technical Conference Proceedings (April 24-29, 2004) Dallas, TX, pp. 96-100.

Fluxes of ions in HIPIMS

786

André Anders J. Vac. Sci. Technol. A, Vol. 28, No. 4, Jul/Aug 2010

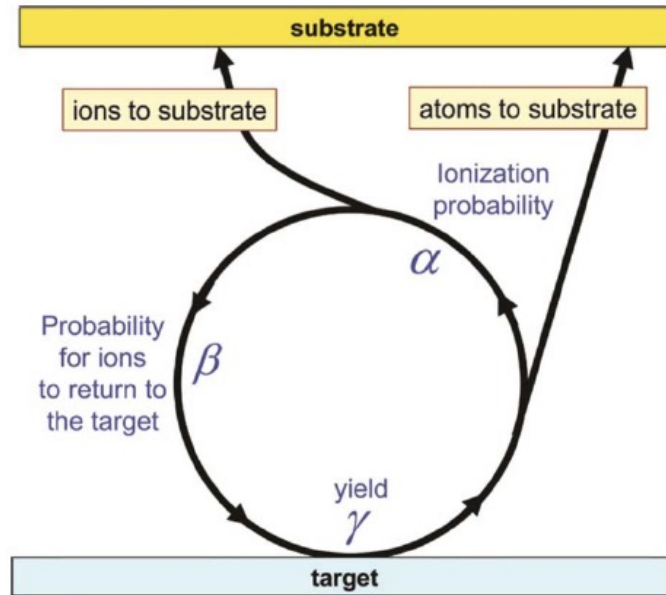


FIG. 2. (Color online) Schematic presentation of the fluxes involved in the deposition by HIPIMS under conditions when the plasma is dominated by metal sputtered from the target; α , β , and γ are the ionization probability, the return probability, and the sputtering yield, respectively; for further explanations see text.

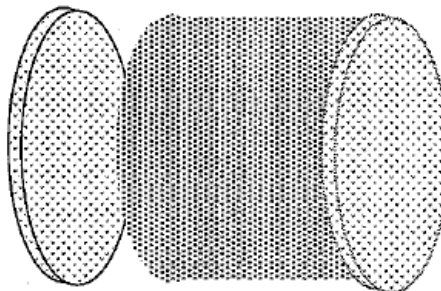
Reactive sputtering

Reactive Sputtering

- Sputtering of an elemental target in the presence of a gas (in addition to the inert gas) that will react with the element to form a compound
 - Examples:
 - Al + O₂ to form Al₂O₃
 - Ti + N₂ to form TiN
 - Purposely add the reactive gas
 - Outgassing can be a factor

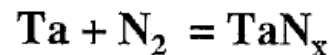
Reactive sputtering

Reactive Sputtering



Target + Reactive gas = Film

1. Doping:



2. Compound formation: $\text{Ta} + \text{O}_2 = \text{Ta}_2\text{O}_5$

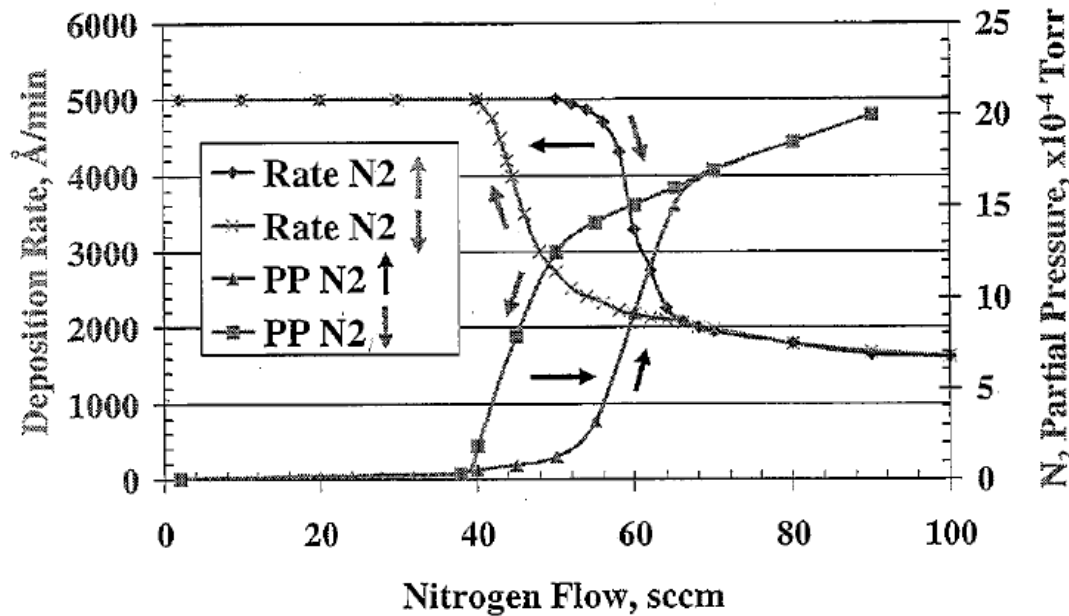
Reactive sputtering

Metal vs. Poisoned Mode

- **Metal mode**
 - Sputtering metal
 - Reactive gas partial pressure low
- **Poisoned mode**
 - Target covered with compound
 - Reactive gas partial pressure high
- **Target can be partially reacted**
 - Takes partial pressure control

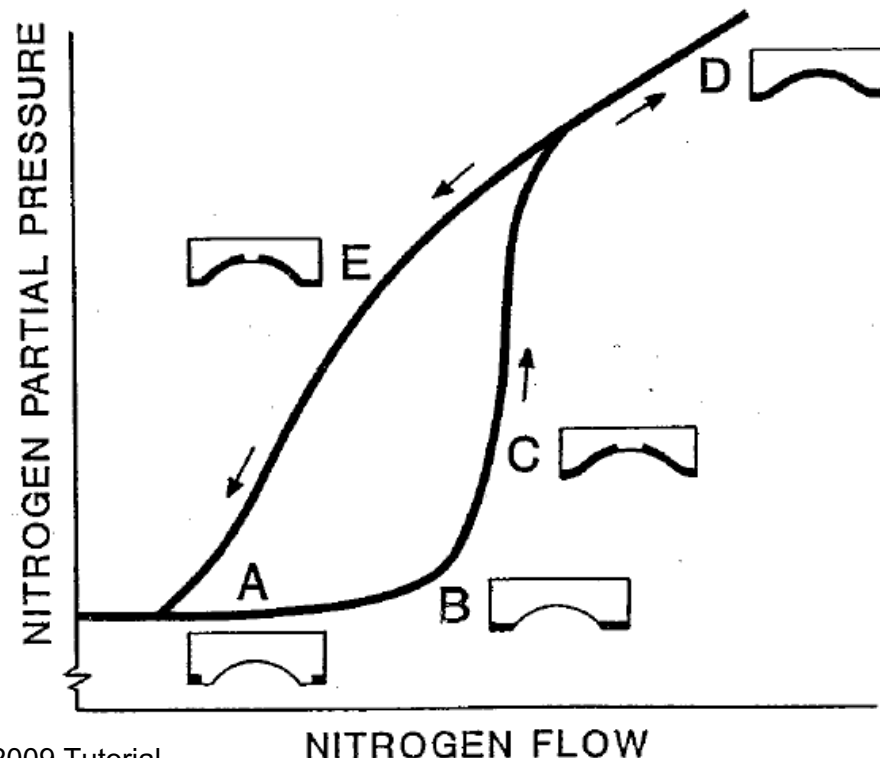
Reactive sputtering

TiN_x Reactive Sputtering: Rate and Hysteresis



Reactive sputtering

Flow Control Hysteresis Loop



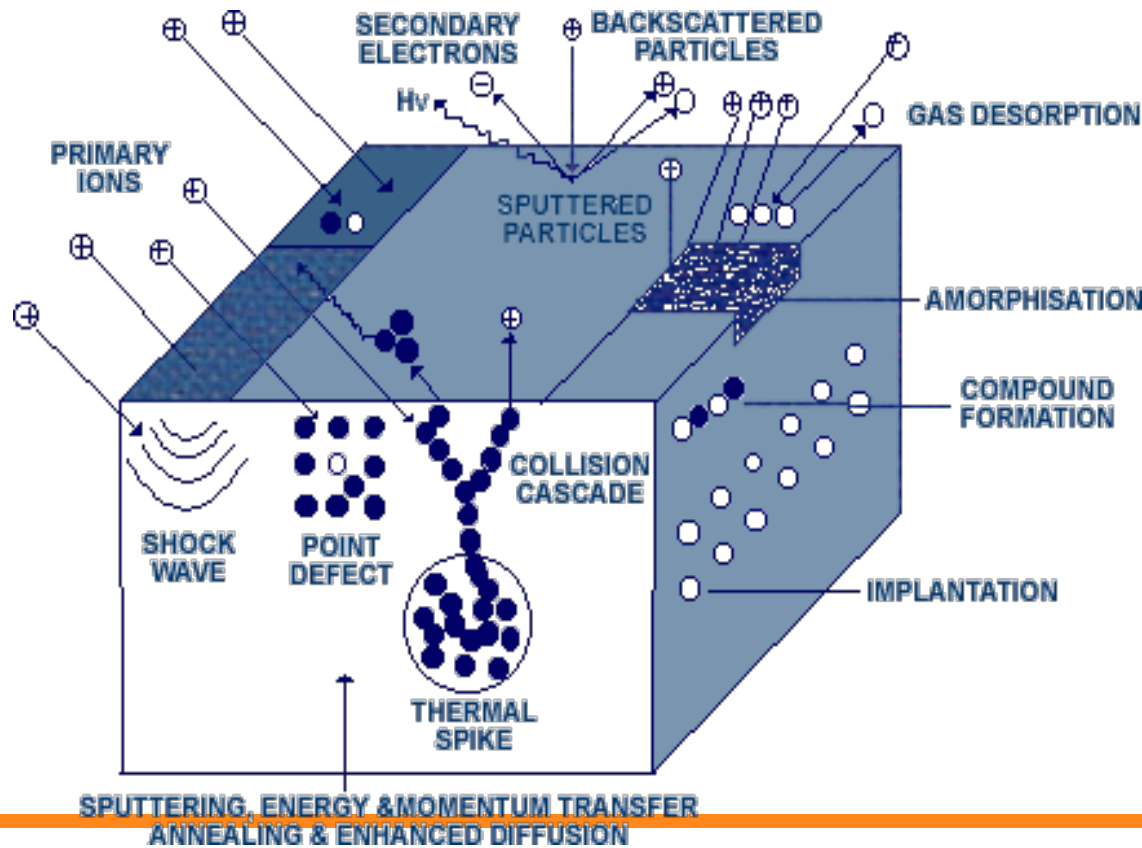
Reactive sputtering

Reactive Deposition Examples

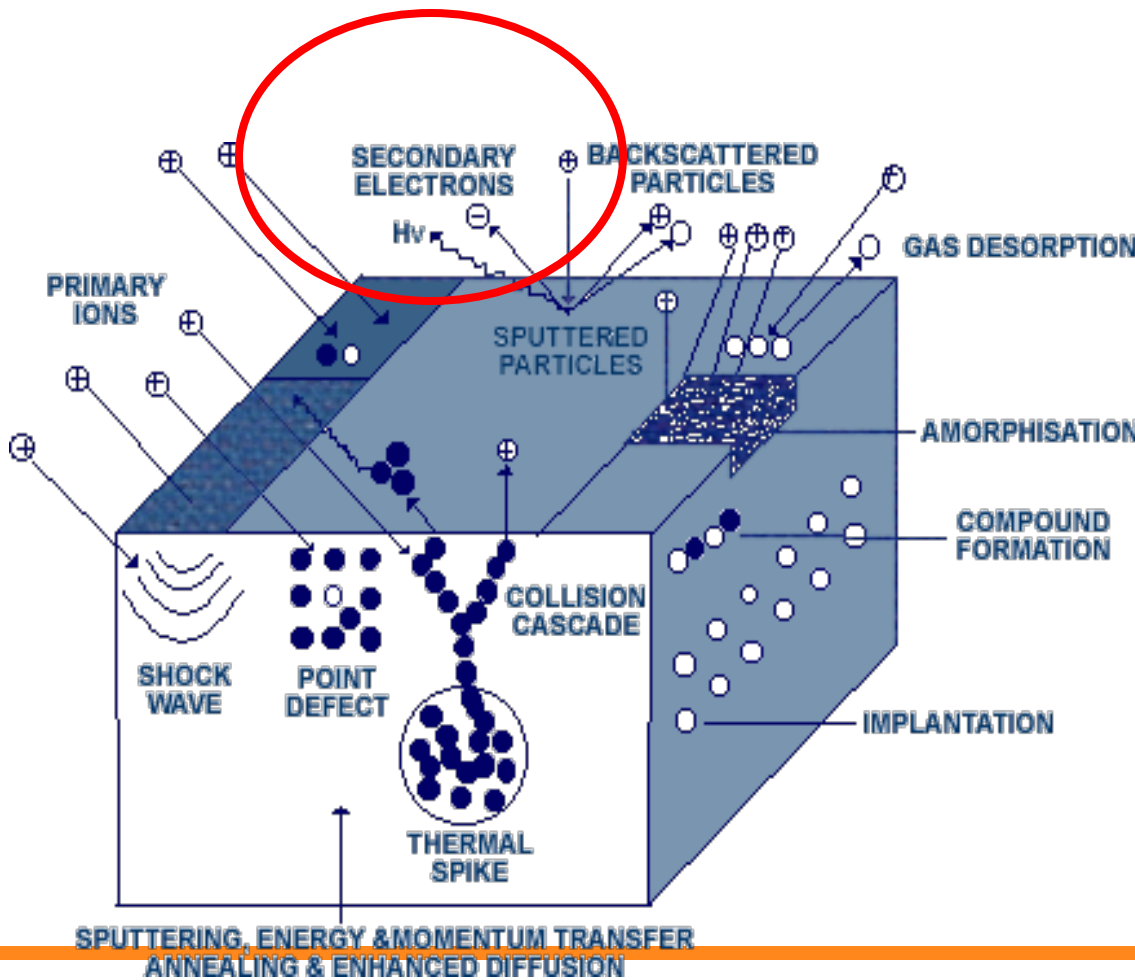
| <u>Target</u> | H ₂ | N ₂ | O ₂ | H ₂ S | AsH ₃ | Ga(CH ₃) |
|-------------------------------------|----------------|--------------------------------|--------------------------------|-------------------|------------------|----------------------|
| Al | | AlN | Al ₂ O ₃ | | | |
| Ti | TiH | TiN | TiO ₂ | | | |
| Ta | TaH | Ta ₂ N, TaN | Ta ₂ O ₅ | | | |
| Cu | | | CuO | Cu ₂ S | | |
| B | | BN | | | | |
| C | | CN | | | | |
| Si | Si:H | Si ₃ N ₄ | SiO ₂ | | | |
| In _{0.9} Sn _{0.1} | | | ITO | | | |
| Zn | | | ZnO | | | |
| Sb | | | | | GaSb | |
| LiNbO ₃ | | | LiNbO ₃ | | | |
| GaAs | | | | | GaAs | |
| ZnO | | ZnO _{1-x} | ZnO | | | |

Ion solid interarctions

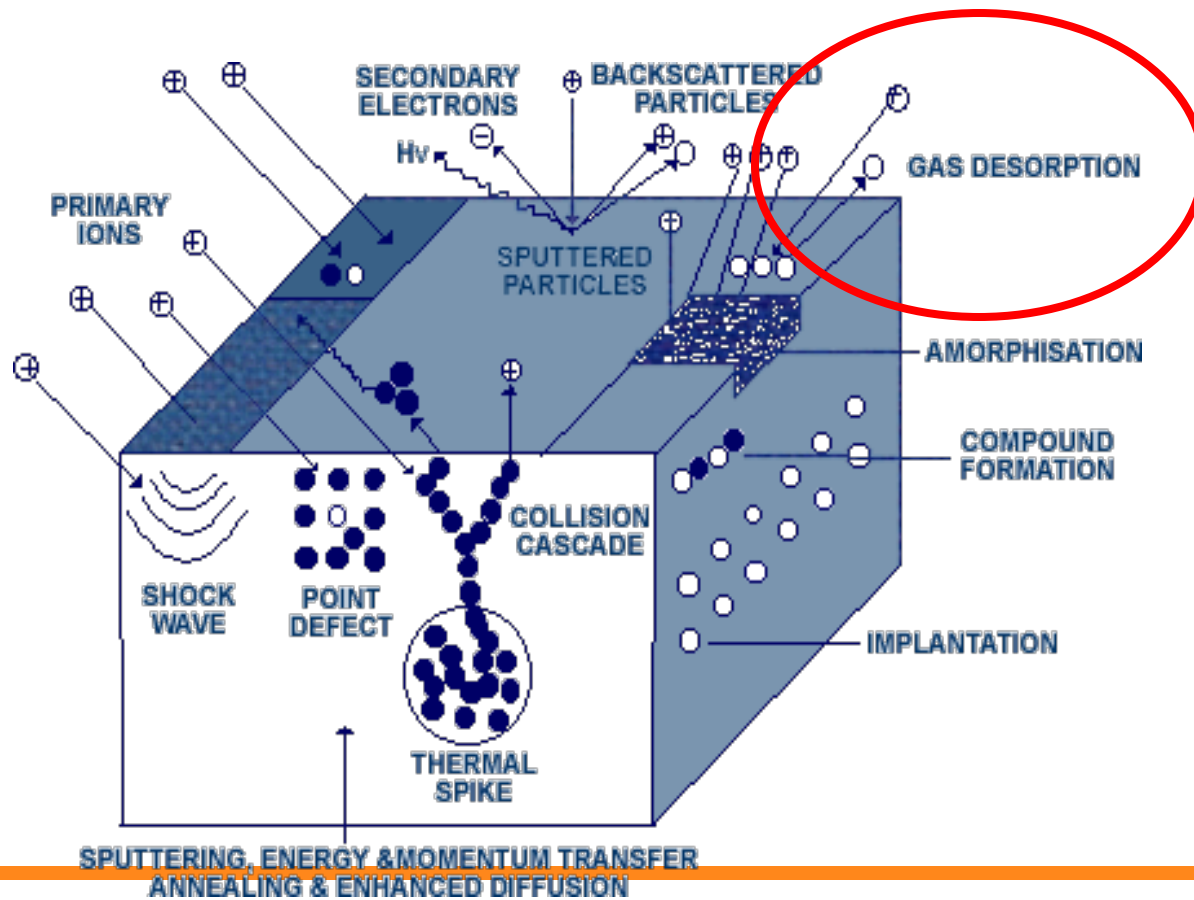
Energetic ion surface interactions



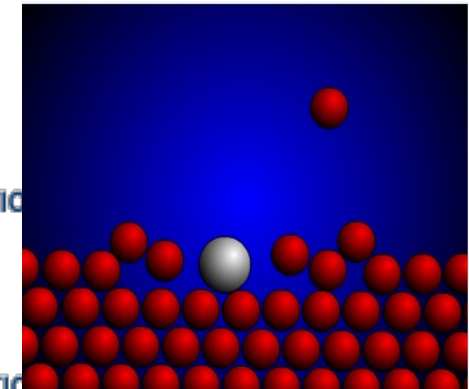
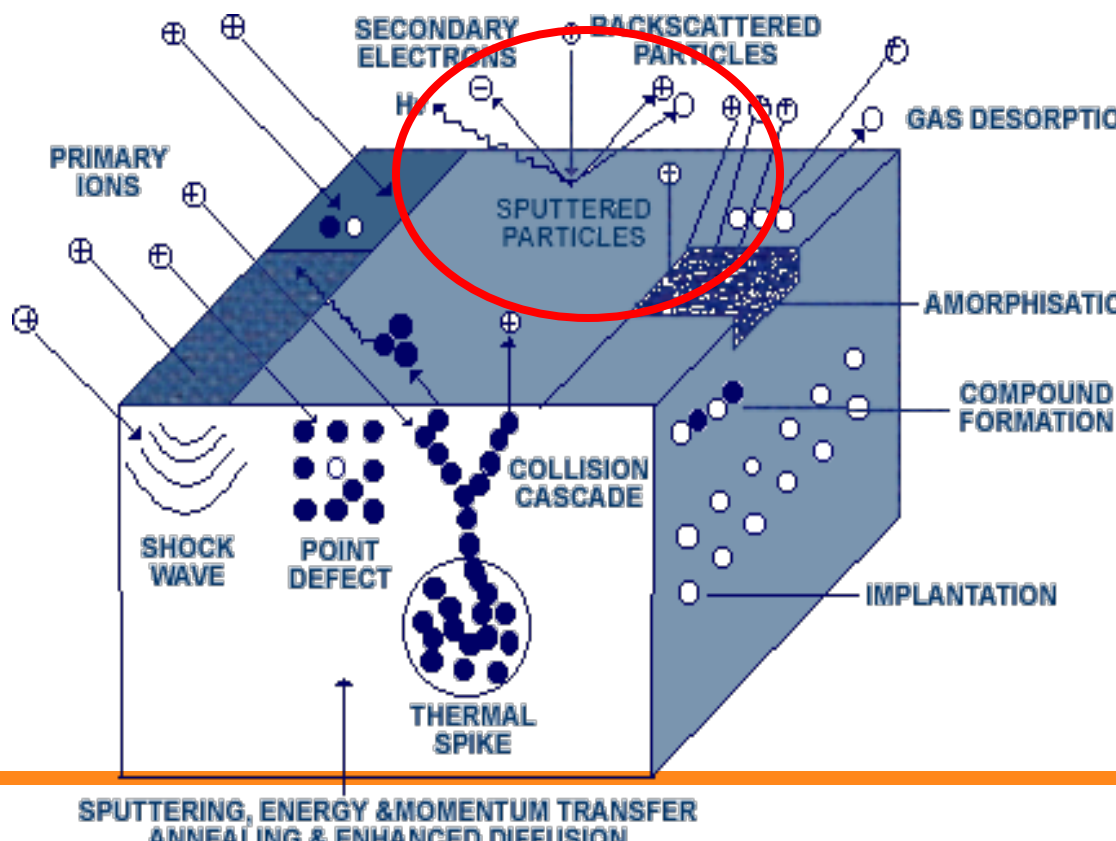
Secondary electrons



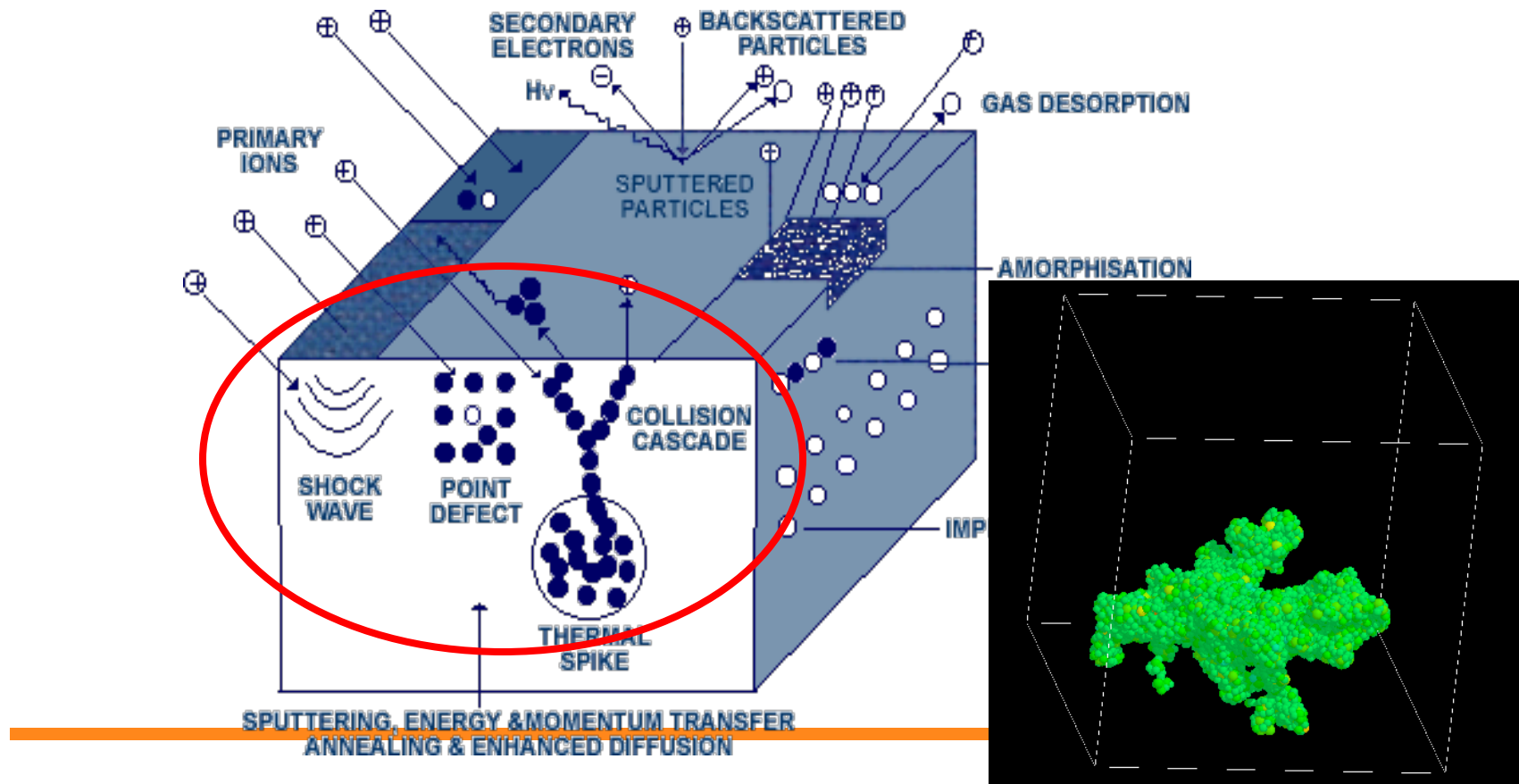
Desorption, cleaning



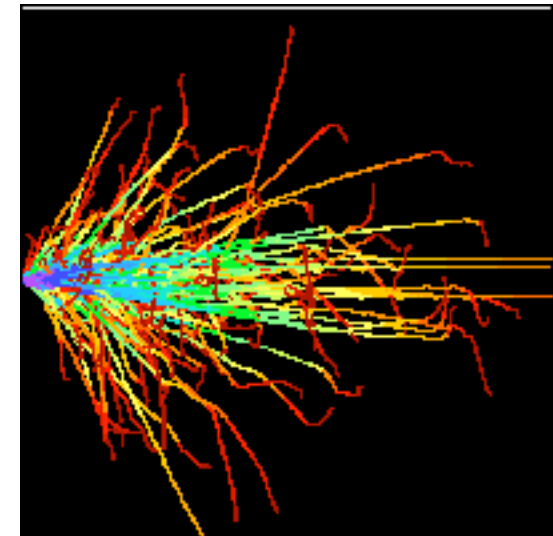
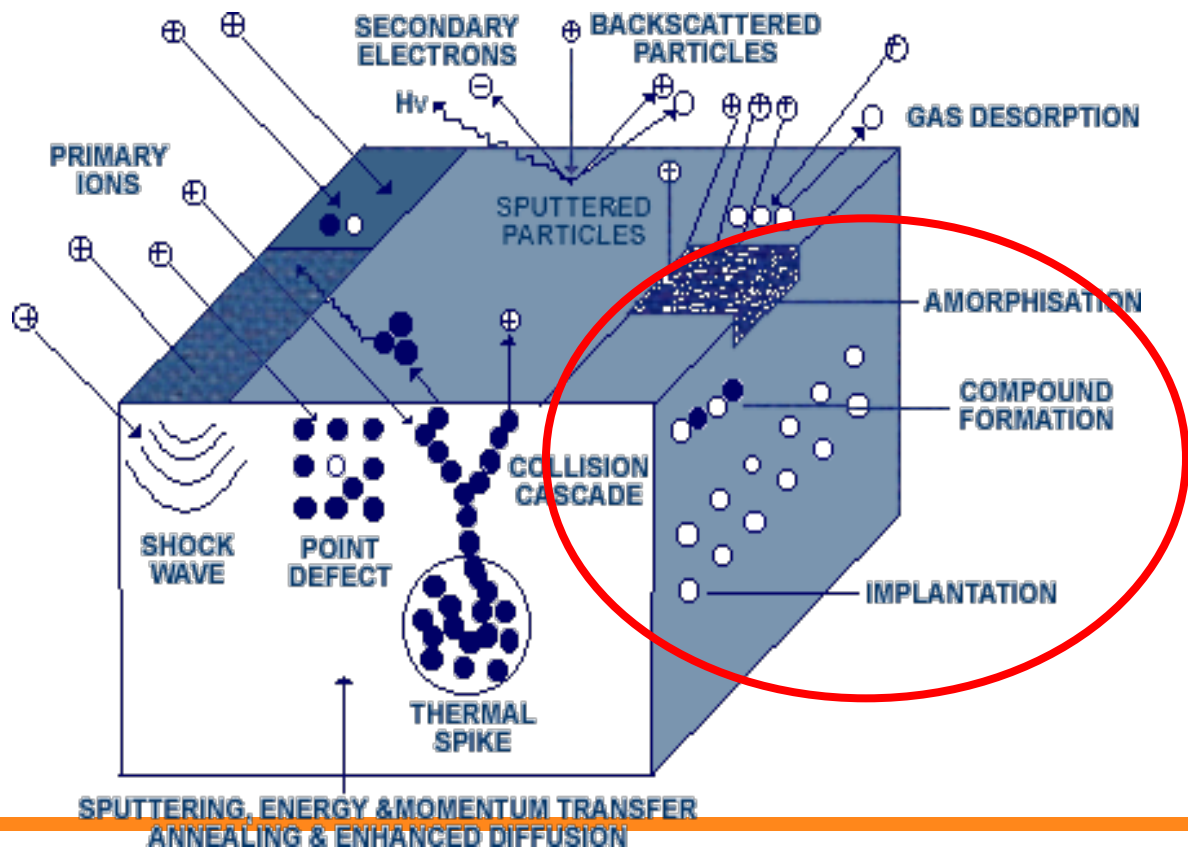
Sputtering



Collision cascade, thermal spike

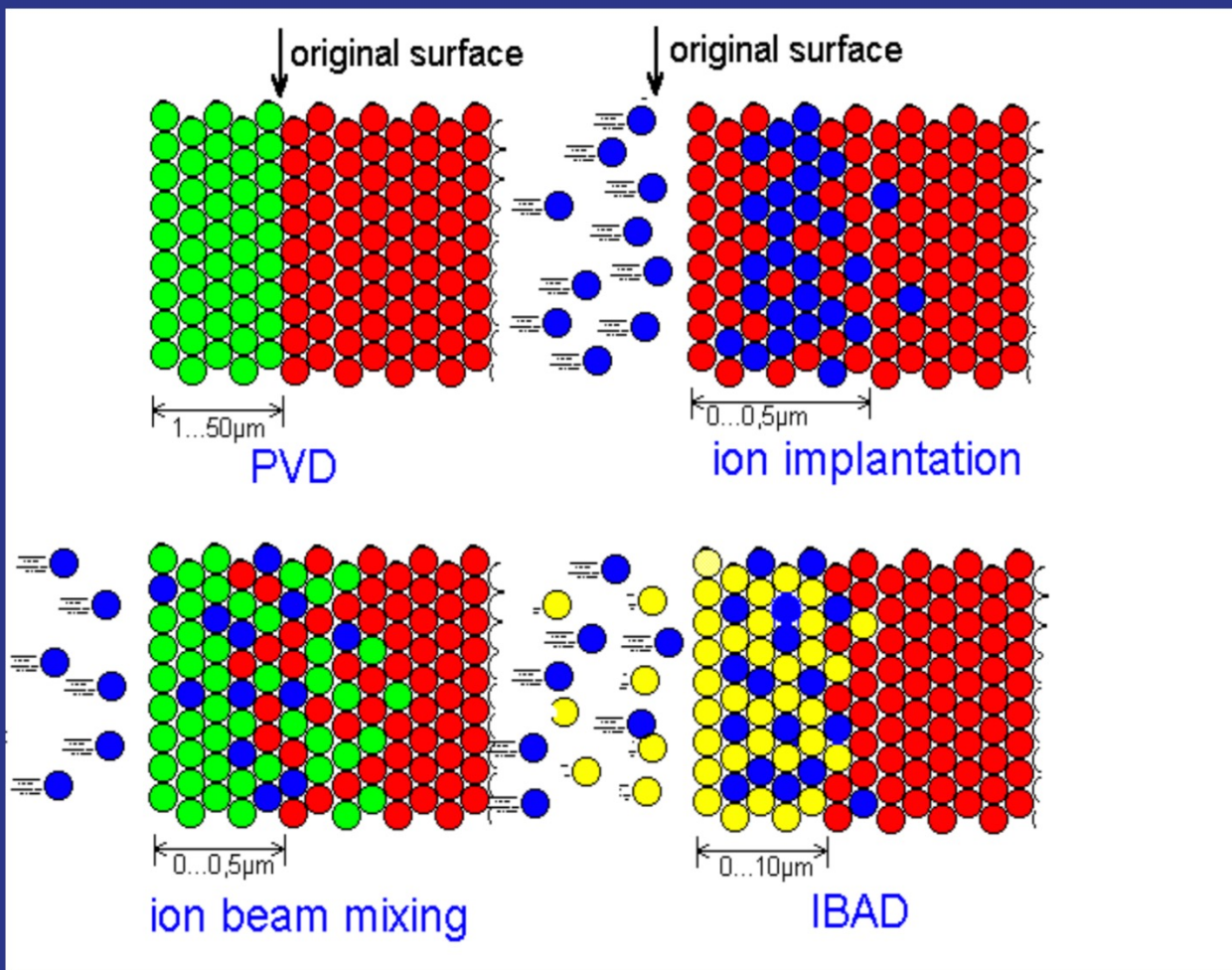


doping, compounds



PVD and Ion Assisted Processes

Which role can energetic ions play



Sputtering

- Source of atoms and ions
- Cleaning: Removing lose atoms, impurities, oxides

Sigmund Theory

$$S = \frac{3\alpha 4M_1 M_2 E}{4\pi^2 (M_1 + M_2)^2 U_s}$$

Good for low energy (<1keV)

where :

α is a function of $M(\text{target})/M(\text{ion})$ and

incident angle $0.1 > \alpha > 1.4$

but often has a value of 0.2 - 0.4

M_1 is the Mass of the ion

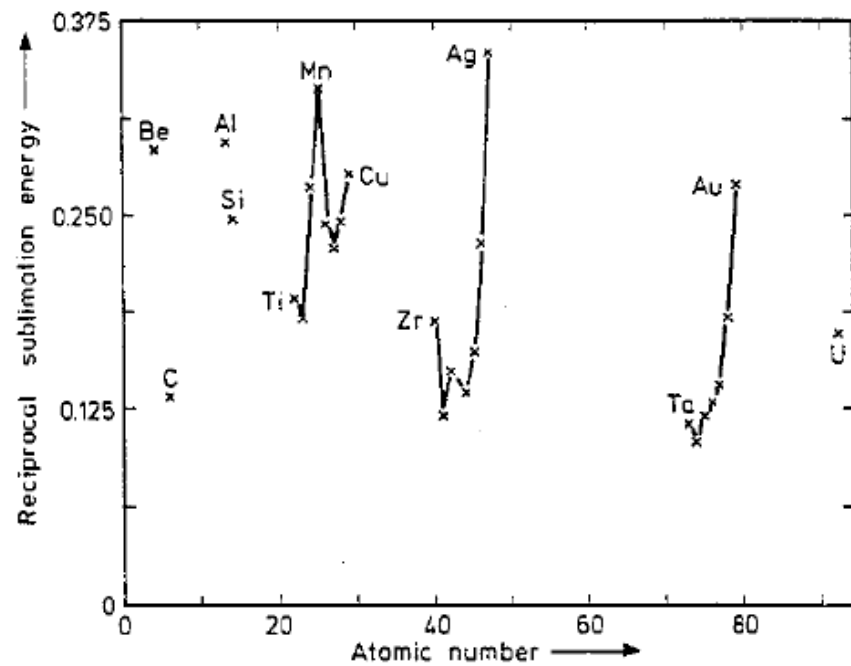
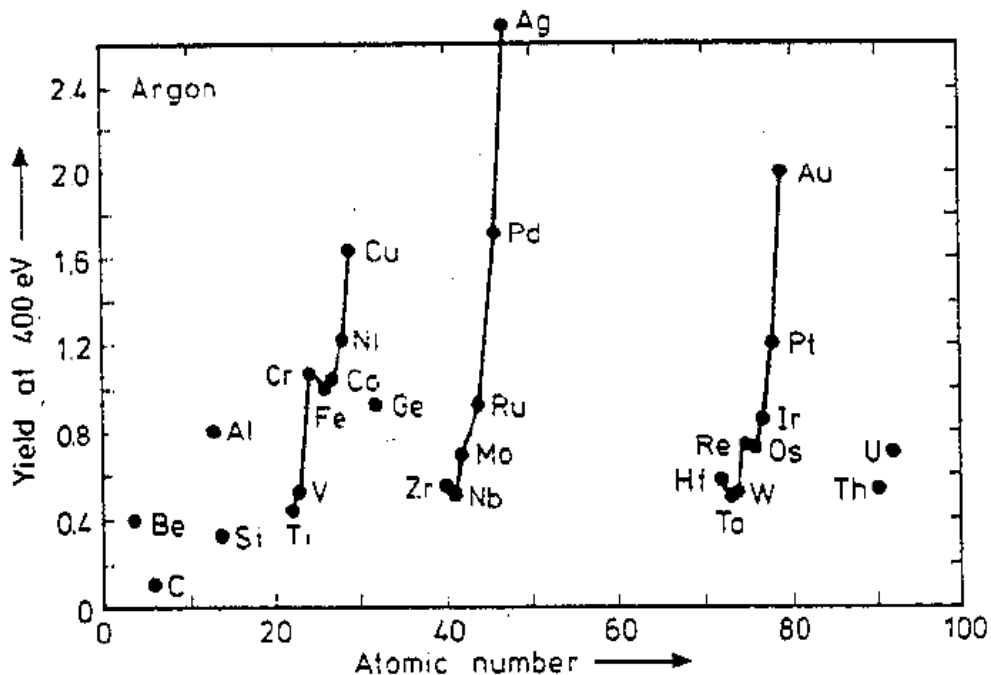
M_2 is the mass of the target

E is incident ion energy

U_s is the binding energy of the target ions

Sputter yield and sublimation energy

$$N(E) \propto \frac{E}{(E + U_0)}$$



Sputter yield angle dependence

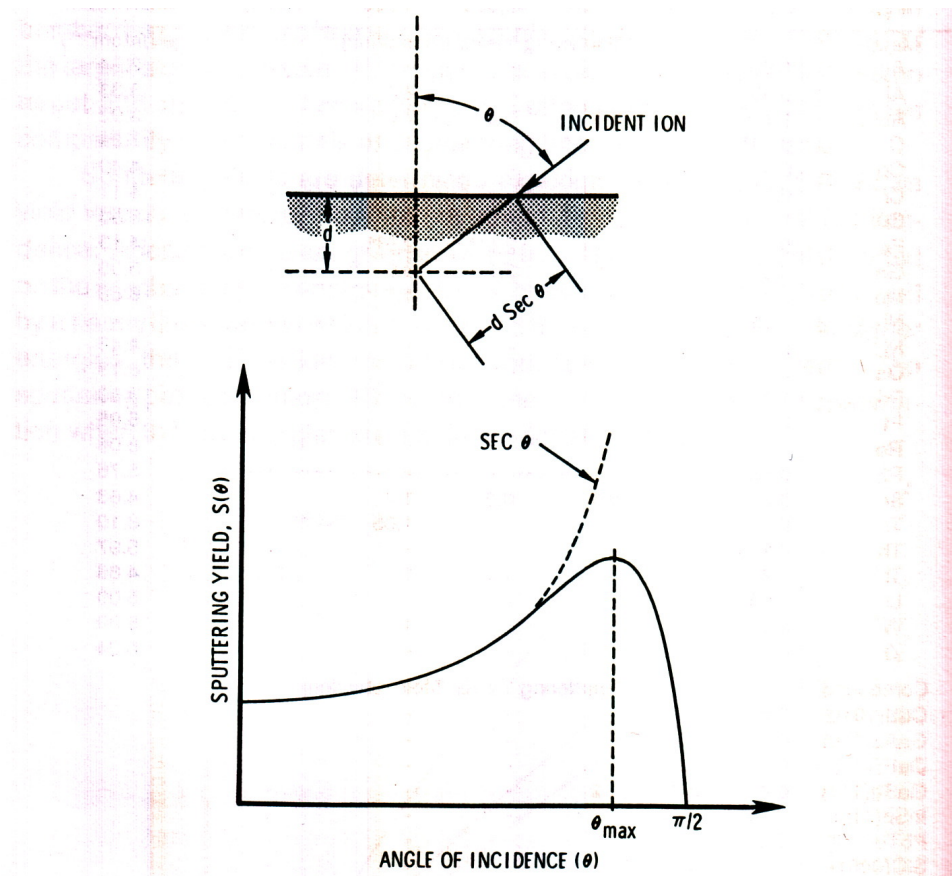
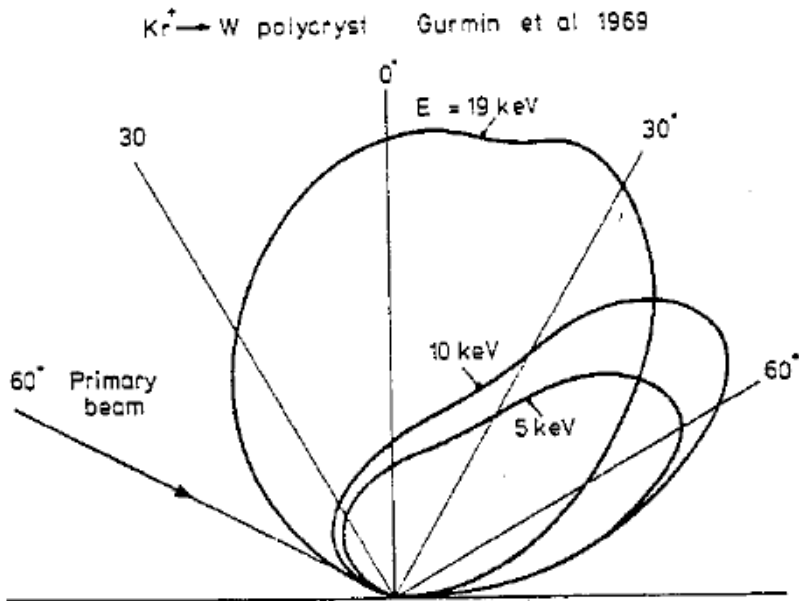


Figure 5.7. Schematic diagram showing variation of the sputtering yield with ion angle of incidence for a constant ion energy.

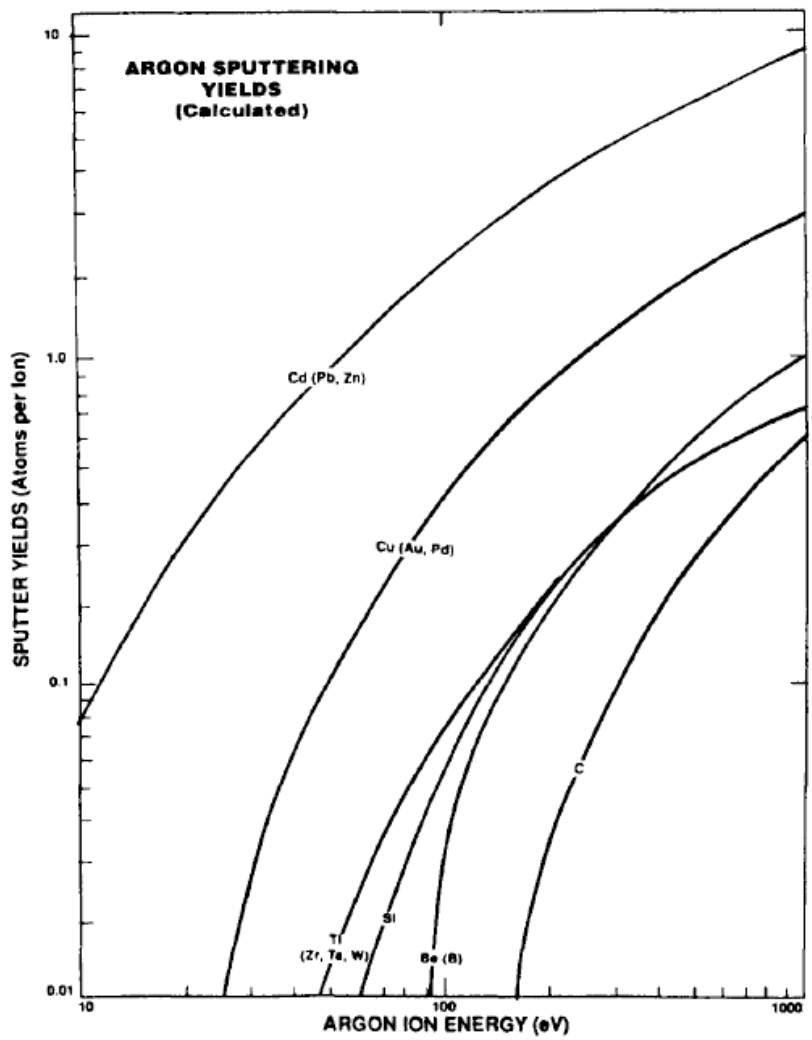
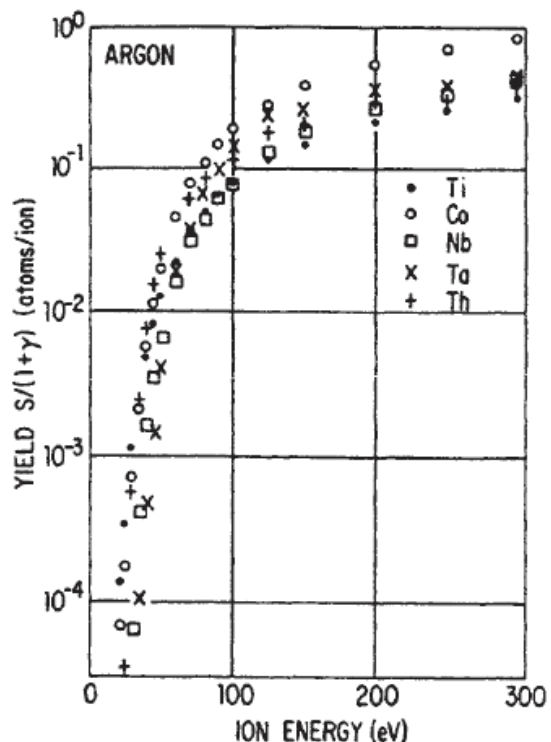
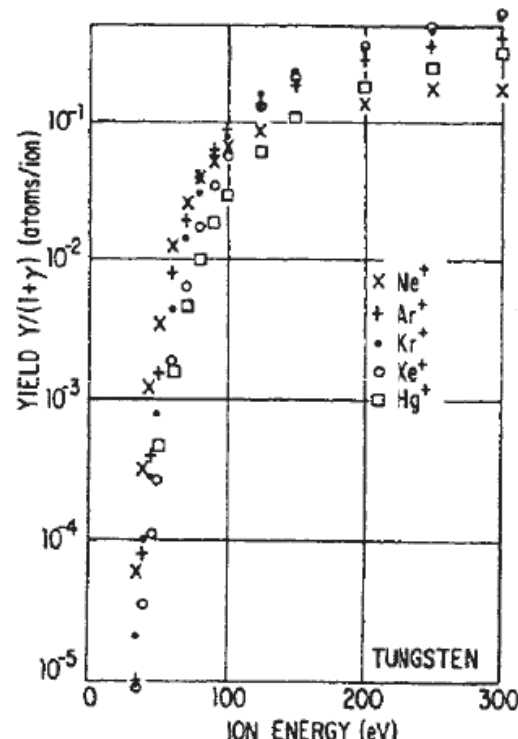


Figure 6-3. Some calculated sputtering yields (adapted from Ref. 20).

Sputter yield angle dependence and energy distribution



(a)



(b)

Figure 3. Sputter yield, S , vs ion energy; (a) shown for several materials with Ar^+ bombardment, and (b) for W bombarded by different ion species.^[10] (Reproduced with permission from Maissel and Glang, Handbook of Thin Film Technology, McGraw-Hill, 1970.)

Preferential sputtering

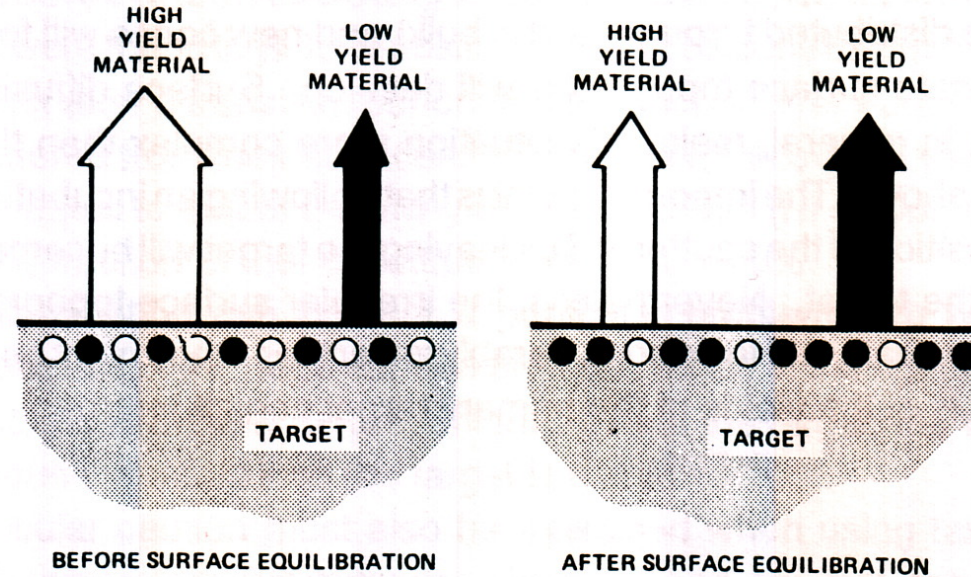


Figure 5.10. Schematic illustration of the surface composition modification which occurs during sputtering of a single-phase alloy.

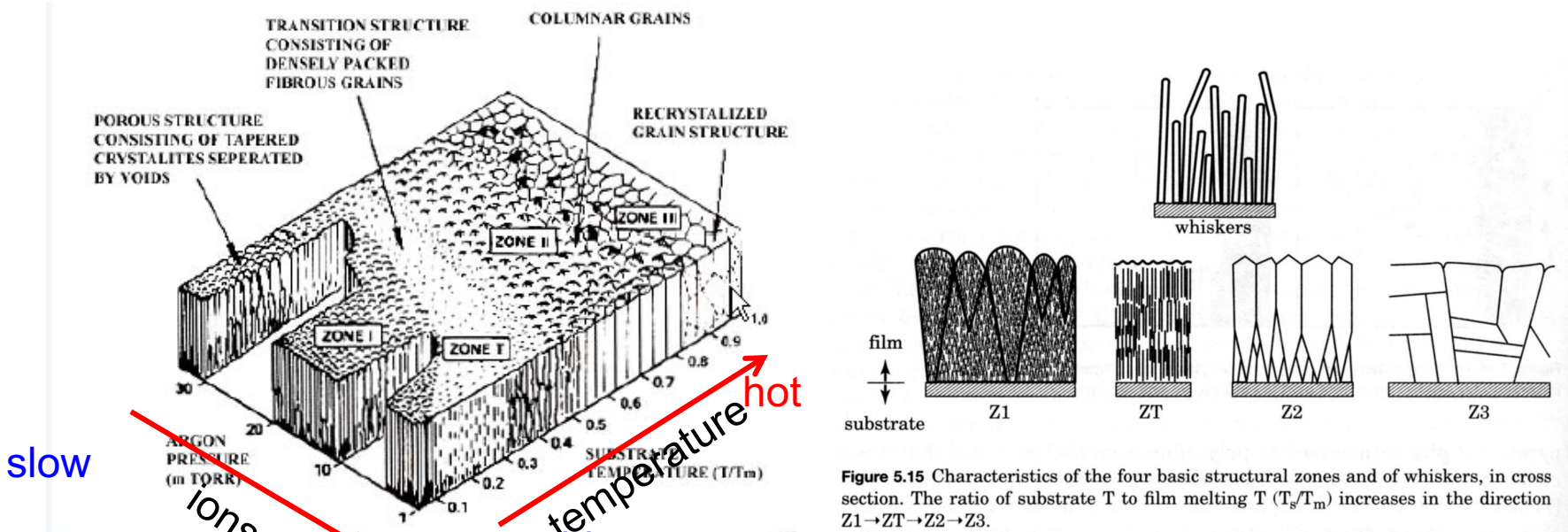
Adatom nucleation and surface diffusion processes

- Shadowing
- Surface diffusion
- Bulk diffusion
- Desorption

Effecting parameters

- kinetic energy, energy of ions and atoms
- thermal energy
- potential energies
- angle of incidence, topography
- impurities – contamination

Coating structure and plasma parameters



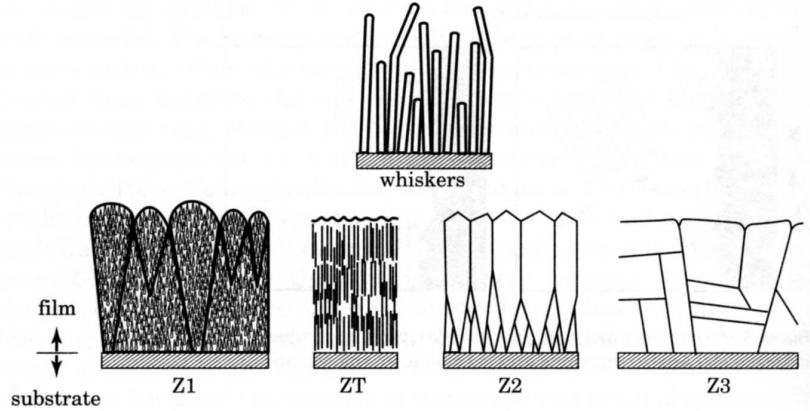


Figure 5.15 Characteristics of the four basic structural zones and of whiskers, in cross section. The ratio of substrate T to film melting T (T_s/T_m) increases in the direction $Z1 \rightarrow ZT \rightarrow Z2 \rightarrow Z3$.

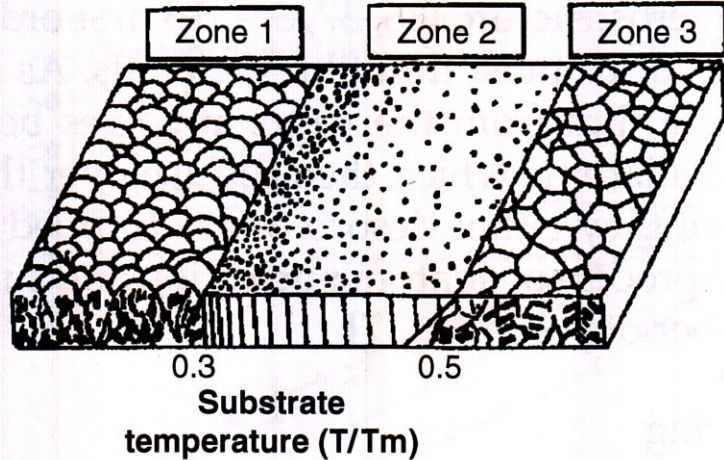


Figure 3.26 Structure zone model of Movechan and Demchishin [39].

Zone 1

- atomic shadowing, low mobility of atoms, continued nucleation
- fibrous grains, pointing at direction of arriving vapor flux, ending with domes shape
- high density of lattice imperfections and pores at grain boundaries
-

Shadow effect

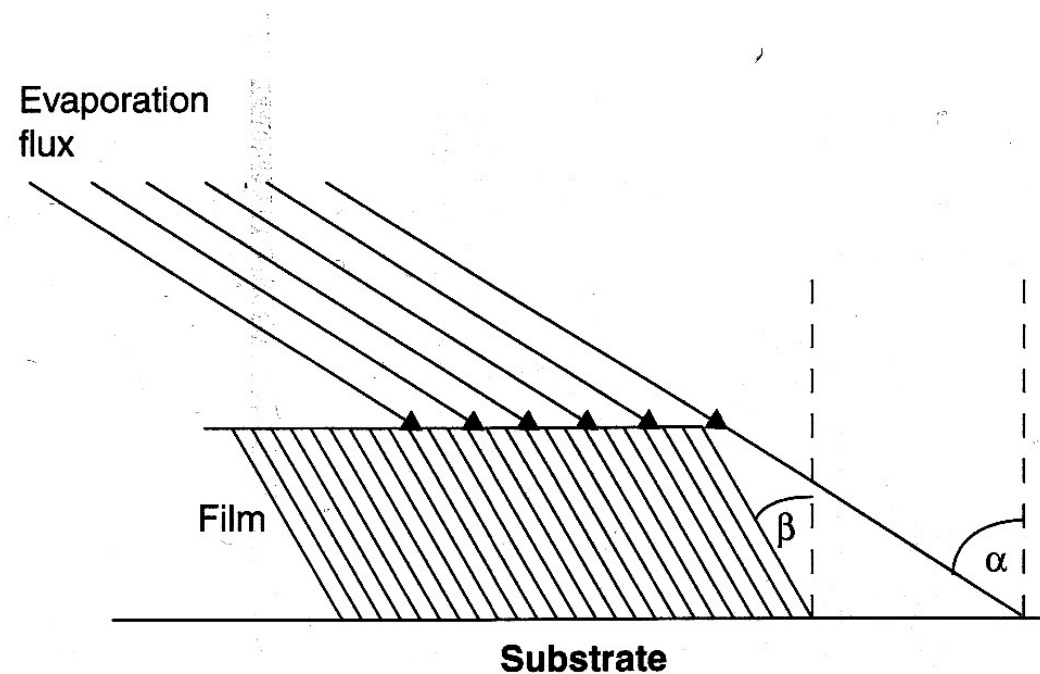


Figure 3.20 Geometry used in the tangent rule [29].

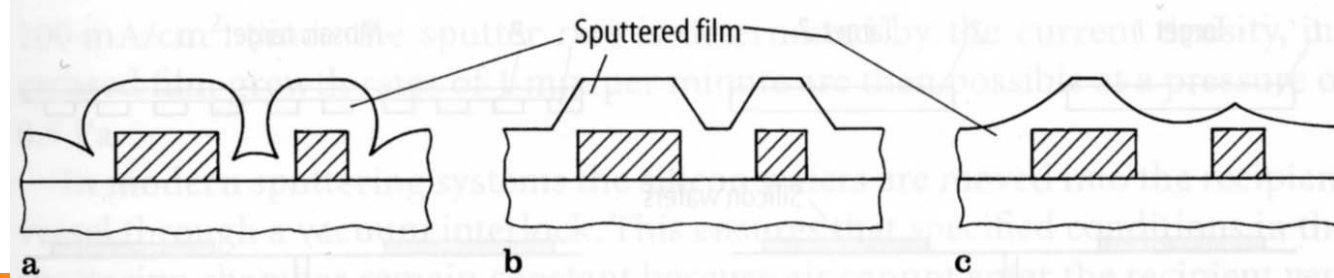


Fig. 3.1.19a-c. Edge coverage of sputtered layers: a no bias; b moderate bias; c heavily biased

Structural hierarchy

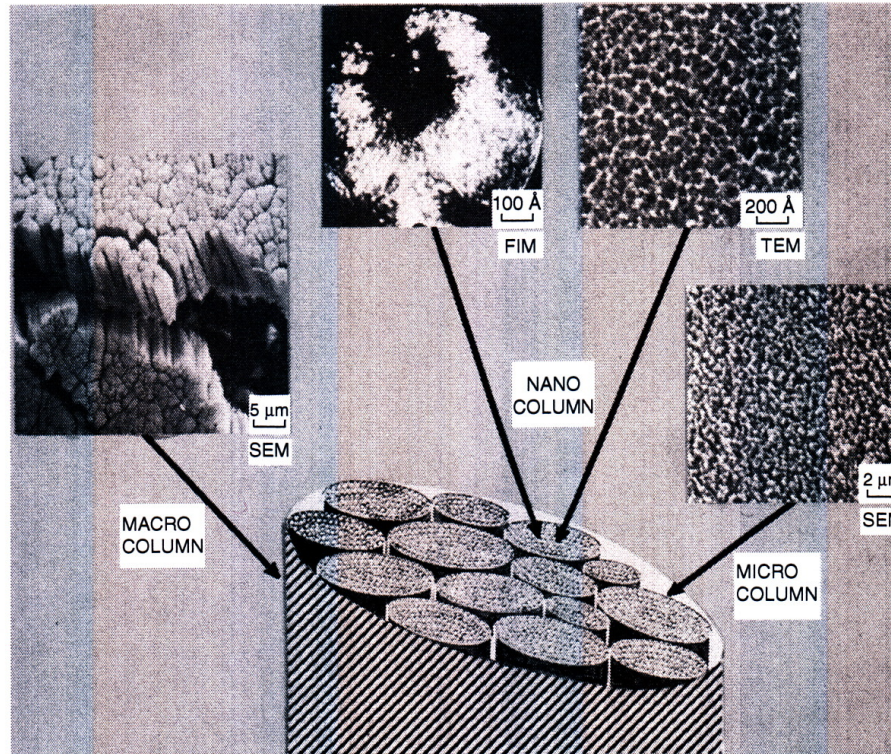


Figure 3.22 Physical structure of nano-, micro and macro columns in a-Ge films [31].

Nodules

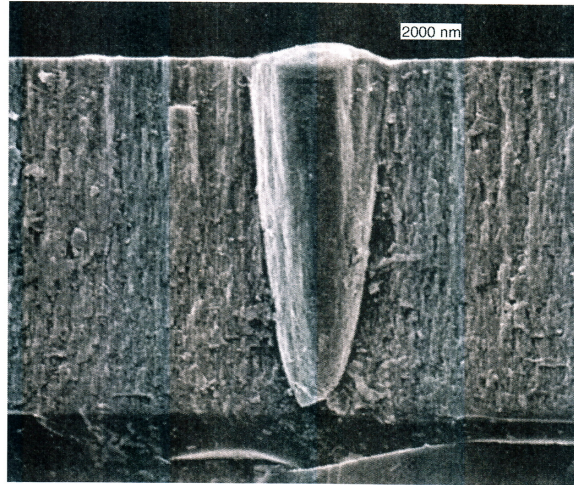


Figure 3.23 Nodule in an AlON rugate filter [28].

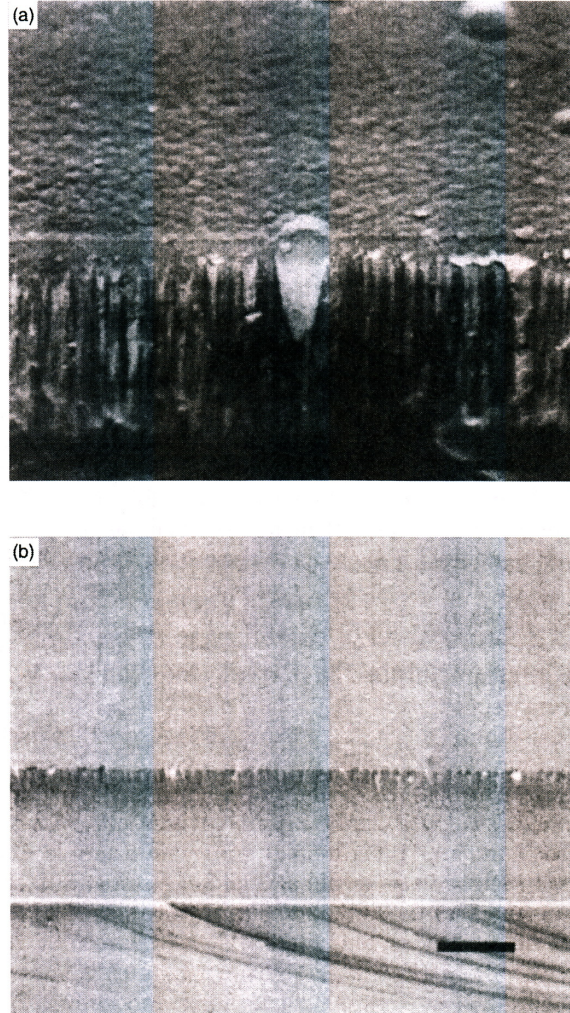


Figure 3.21 SEM micrograph of two SiC films; film (a) had no ion bombardment and film (b) was exposed to ion bombardment [31].

GLAD

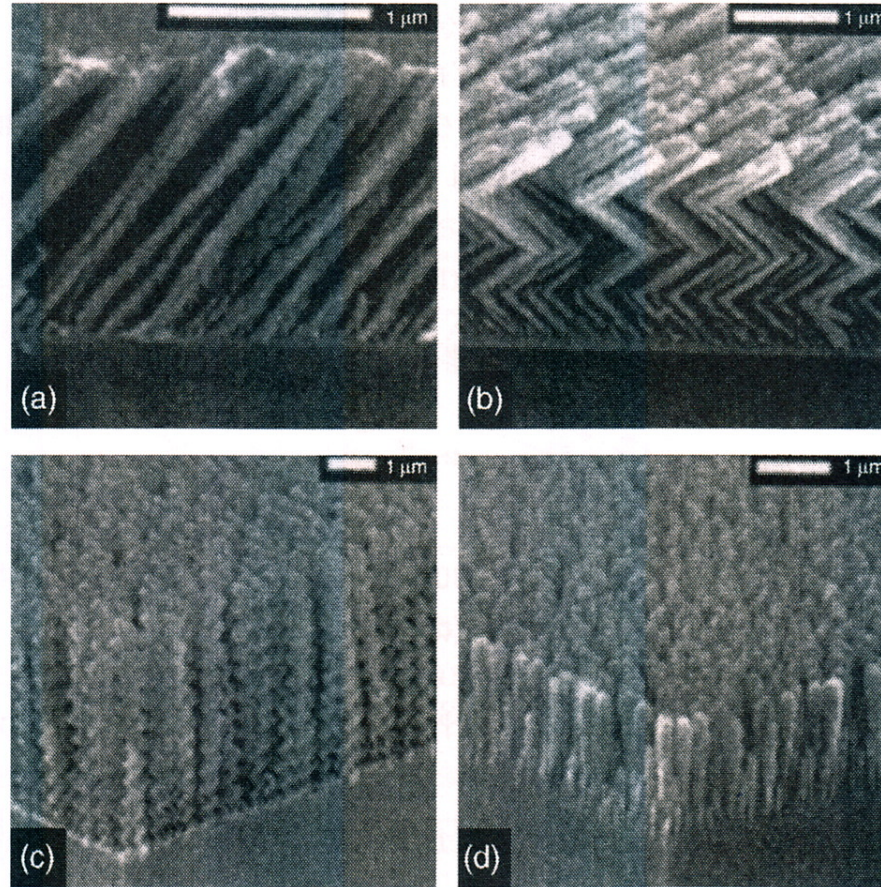


Figure 3.24 Columnar structures fabricated using the GLAD process [32].

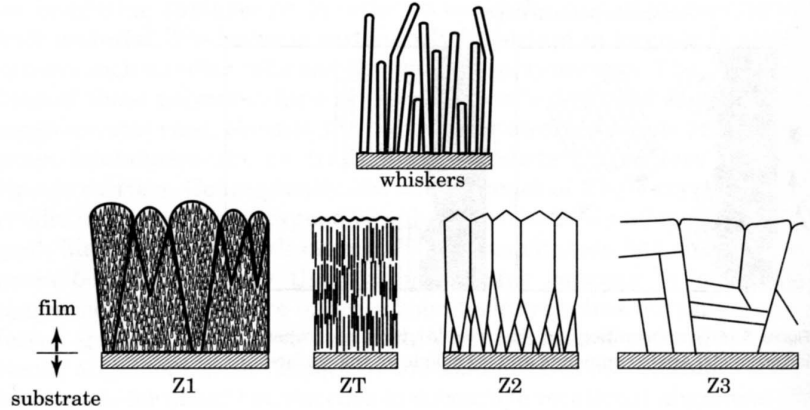


Figure 5.15 Characteristics of the four basic structural zones and of whiskers, in cross section. The ratio of substrate T to film melting T (T_s/T_m) increases in the direction $Z1 \rightarrow ZT \rightarrow Z2 \rightarrow Z3$.

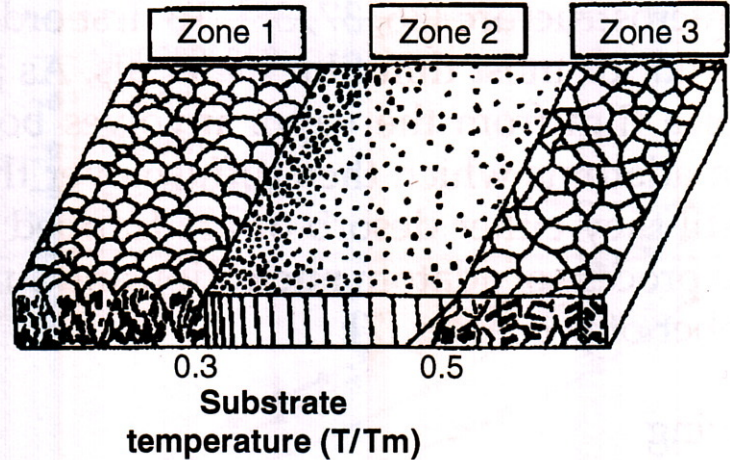


Figure 3.26 Structure zone model of Movechan and Demchishin [39].

Zone 2

- surface diffusion dominates
- uniform columnar grains, grainsize increases with T_h
- faceted surface
- mechanically weak
- electrically favorable e.g. in piezo electrical thin films

Zone T

- transition between zone1 and 2 surface diffusion is “remarkable”
- grain boundary diffusion is limited
- competitive grain growth of V-shaped crystals
- mechanically favorable

Competition of growing crystals

Handbook of Deposition Technologies for Films and Coatings - Science, Applications and Technology (3rd Edition)
Edited by: Martin, Peter M. © 2010 William Andrew Publishing

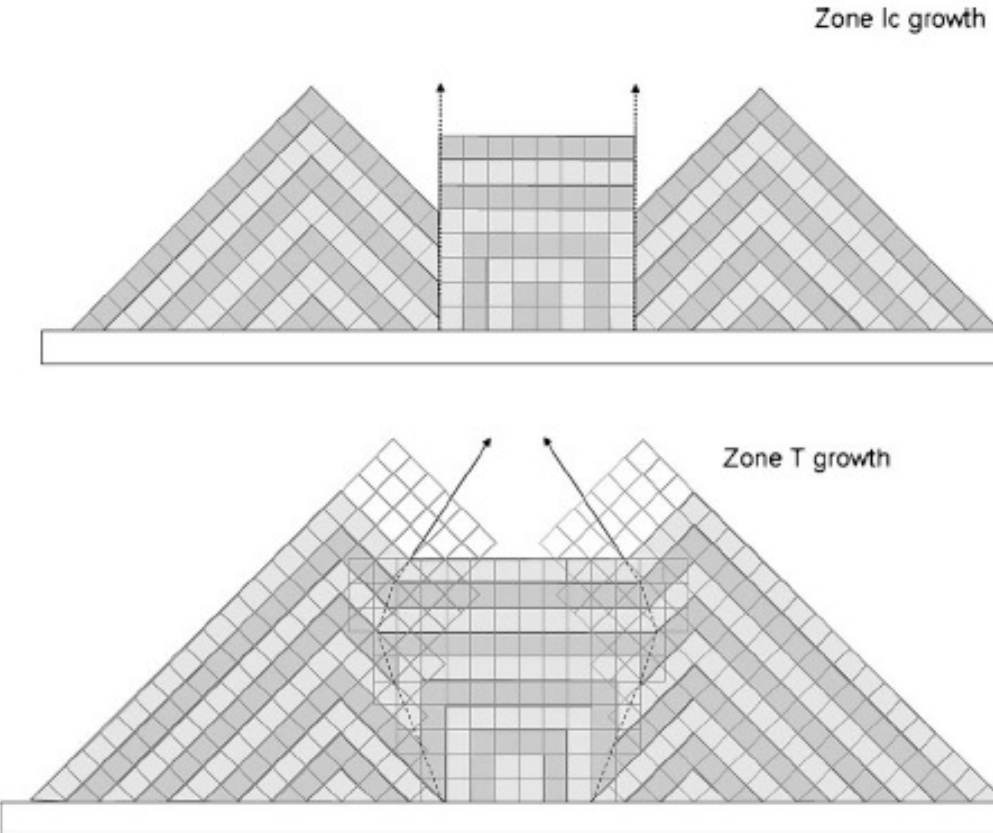


Figure 5.21: Schematic comparison between zone lc and zone T growth. To indicate the identical normal growth rate of the planes of both grains, alternating coloring is used. In zone T, an overgrowth of one grain by an adjacent grain is observed.

Columnar growth

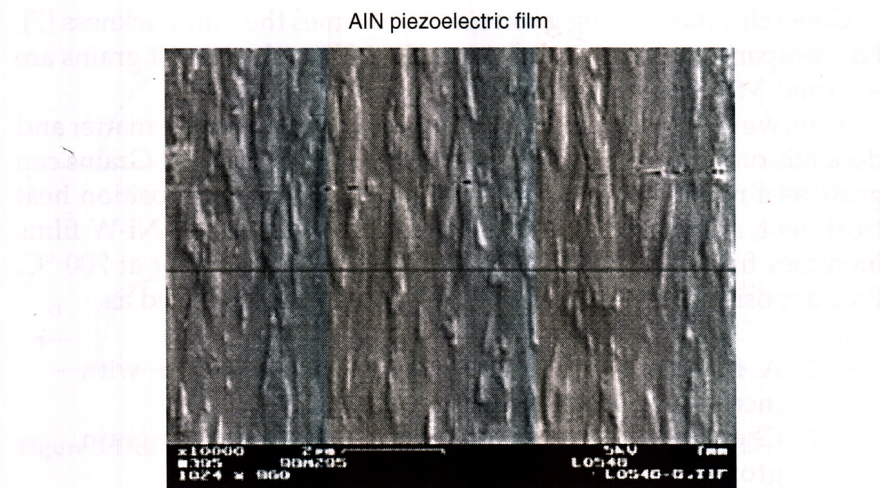


Figure 3.18 SEM picture of well-behaved columnar thin film microstructure.

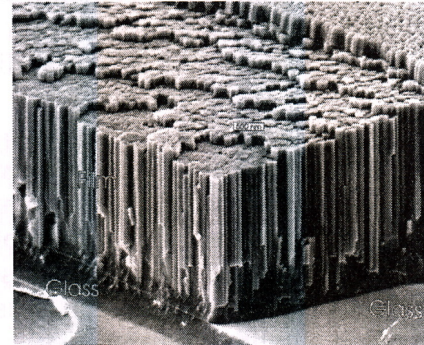


Figure 3.19 Columnar structure in an RF sputtered ALON film [28].

Columnar crystals



15.4.2011 Koskinen

Columnar crystals



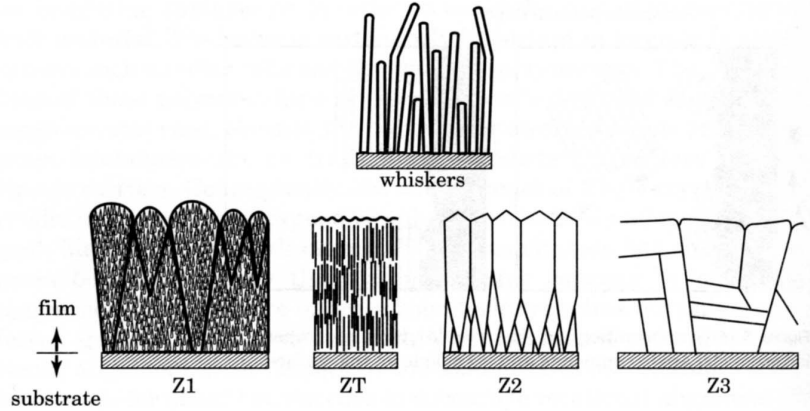


Figure 5.15 Characteristics of the four basic structural zones and of whiskers, in cross section. The ratio of substrate T to film melting T (T_s/T_m) increases in the direction $Z1 \rightarrow ZT \rightarrow Z2 \rightarrow Z3$.

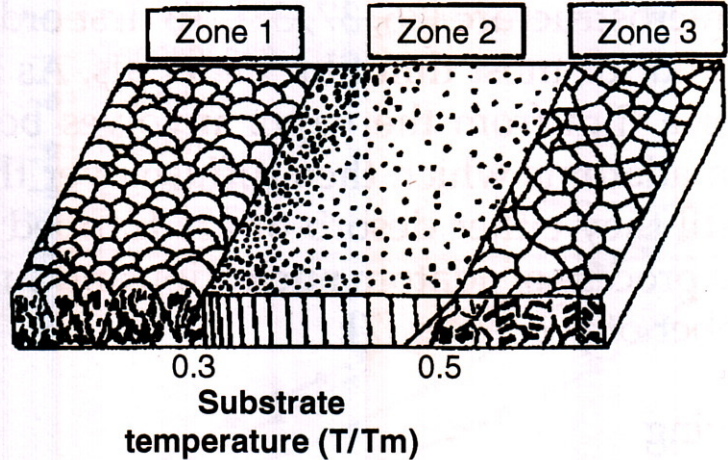


Figure 3.26 Structure zone model of Movechan and Demchishin [39].

Zone 3

- bulk diffusion dominates
- recrystallization of large crystals

Effect of ion energy

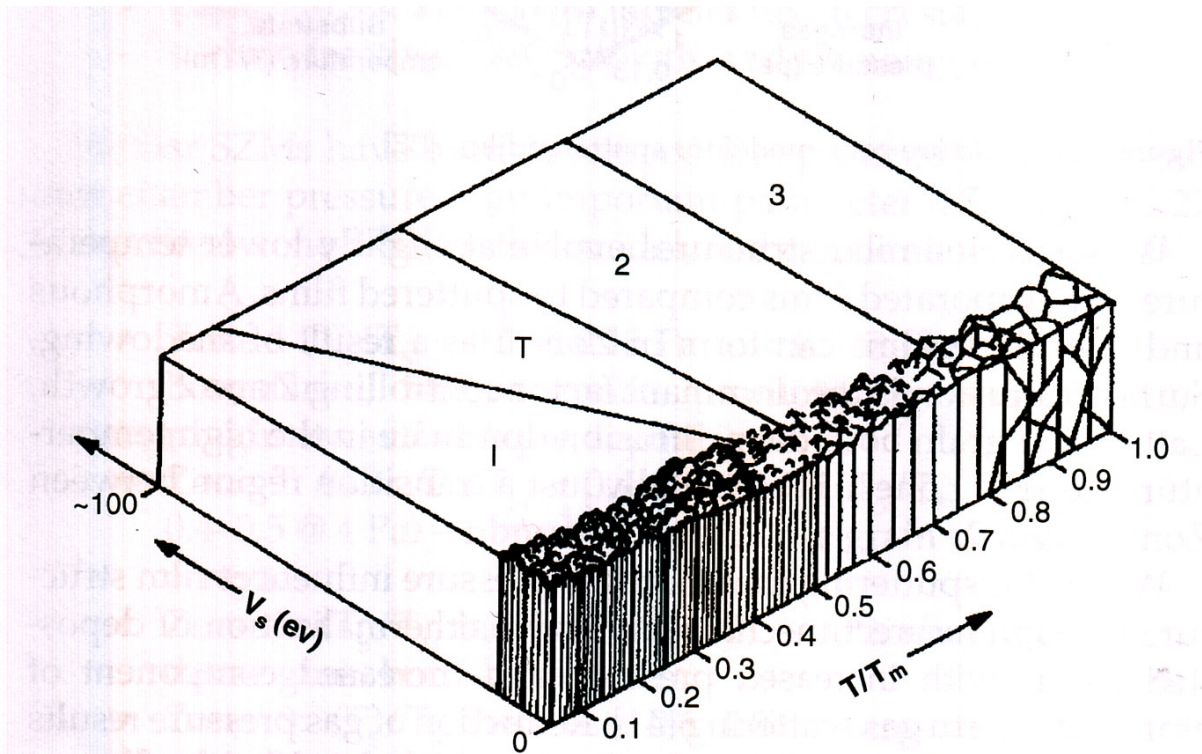


Figure 3.28 Revised SZD for RF sputtering, including ion bombardment.

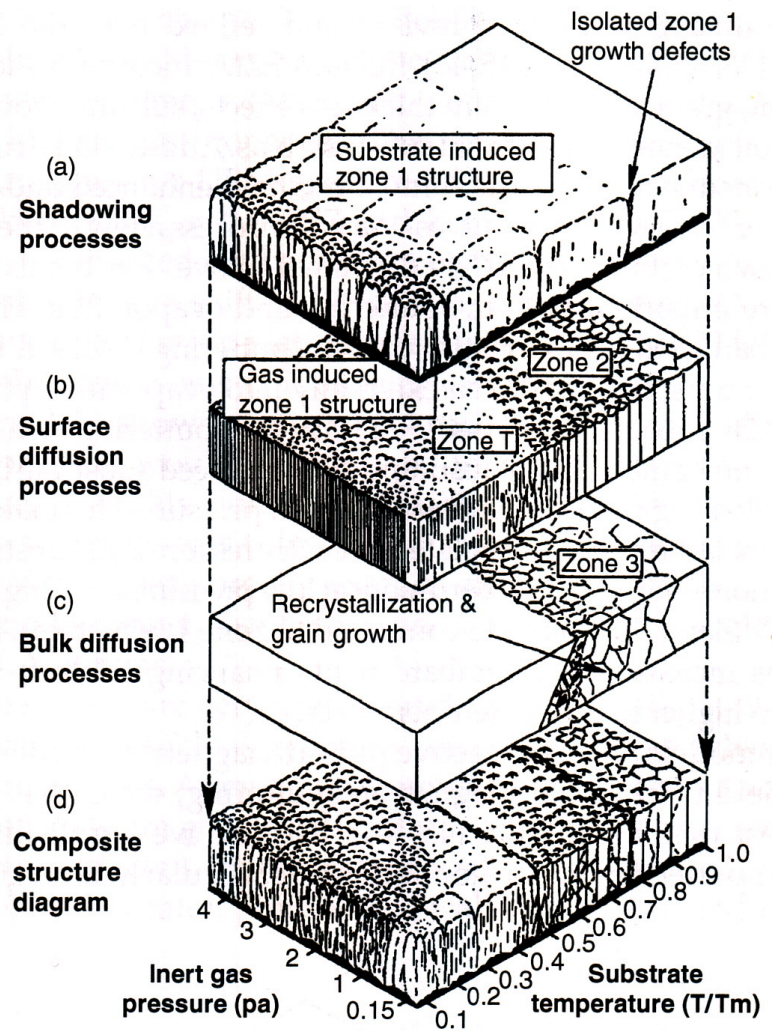
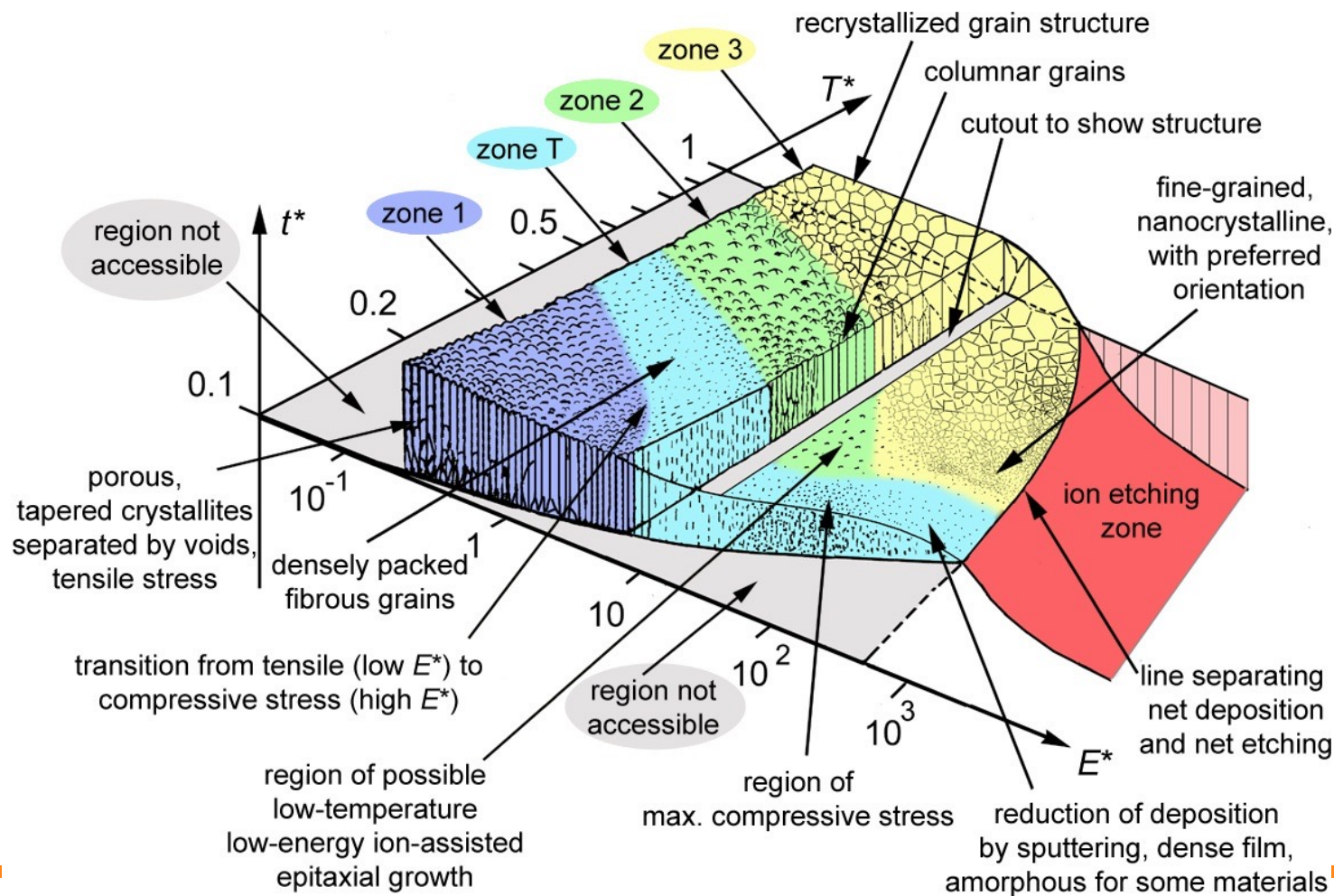


Figure 3.27 Structure zone model for sputtered films [37].

Generalize parameters to all PVD processes

- Replace the linear T_h axis with a generalized temperature T^* , which includes the homologous temperature + the temperature shift caused by the potential energy of particles arriving on the surface (i.e., energetic particle and ion bombardment).
- Replace the linear pressure axis with a logarithmic axis for a normalized energy E^* , which encompasses displacement and heating effects caused by the kinetic energy of bombarding particles.
- Label the z-axis with a net film thickness t^* which will allow maintenance of film structure while including the effects of thickness reduction by densification and sputtering. Ion etching is included in this quantity.

Modified Thorton diagram



Reduced parameters SZD

- $T^* = T_h + T_{pot}$
- $T_h = T_s/T_m$
- $E_{pot} = E_c + (E_i - \phi)$
- $E_{kin} = E_o + QeV_{sheath}$
- $T_{pot} = E_{pot}/kN_{moved}$
- $t^* = \text{thickness}$

$$E^* = \sum_{\alpha} \frac{E_{kin,\alpha} m_{\alpha}}{E_c m_s} J_{\alpha} \Big/ \sum_{\alpha} J_{\alpha}.$$

- T_s , substrate temperature
- T_m , melting temperature
- E_c heat of sublimation or cohesive energy (1 – 9 eV/atom)
- E_i ionization energy (4 – 10 eV/atom)
- E_{kin} ion kinetic energy
- E_o plasma potential
- V_{sheath} sheath potential
- ϕ electron work function (c. 4 eV)
- J_a , flux of species a
- m_a , mass of incoming atom
- m_s , mass of substrate
- k , Boltzmann constant
- N_{moved} , number of rearranged atoms

TRIM and SRIM simulations

<http://www.srim.org/SRIM/SRIM%2008.pdf>

